

# **FINAL SCIENTIFIC REPORT**

## **Enhanced Geothermal Systems Research and Development: Models of Subsurface Chemical Processes Affecting Fluid Flow.**

**Department of Energy Grant: DE-FG36-04GO14300  
Grant Period: 10/1/2004-12/31/2007**

**PRINCIPAL INVESTIGATOR:**  
**Phone: 858-534-6374**

**Dr. Nancy Moller**  
**Email: [nweare@ucsd.edu](mailto:nweare@ucsd.edu)**

**CO-PRINCIPAL INVESTIGATOR:**  
**Phone: 858-534-3286**

**Professor John H. Weare**  
**Email: [jweare@ucsd.edu](mailto:jweare@ucsd.edu)**

**RECIPIENT ORGANIZATION: University of California, San Diego**  
**Department of Chemistry & Biochemistry**  
**9500 Gilman Drive, La Jolla, CA 92093**

**DOE HQ PROGRAM MANAGER: Allan Jelacic**  
**[allan.jelacic@hq.doe.gov](mailto:allan.jelacic@hq.doe.gov)**

**DOE PROJECT OFFICER: Jay Nathwani, Golden Field Office**  
**[jay.nathwani@go.doe.gov](mailto:jay.nathwani@go.doe.gov)**

## NOTICES

**Acknowledgement:** This report is based upon work supported by the U.S. Department of Energy under Award No. DE-FG36-04GO14300.

**Disclaimer:** Any findings, opinions and conclusions or recommendations expressed in this report are those of the authors and do not necessarily reflect the views of the Department of Energy.

**Proprietary Data Notice:** If there are any patentable material or protected data in the report, the recipient, consistent with data protection provisions of the award, must mark the appropriate block in Section K of the DOE F 241.3, clearly specify it here, and identify them on appropriate pages of the report. Other than patentable material or protected data, reports must not contain any proprietary data (limited rights data), classified information, information subject to export control classification, or other information not subject to release. Protected data are specific technical data, first produced in the performance of the award, which are protected from public release for a period of time by the terms of the award agreement. Reports delivered without notice may be deemed to have been furnished with unlimited rights, and the Government assumes no liability for the disclosure, reproduction or use of such reports.

## TABLE OF CONTENTS

SUBJECT	PAGE
Notices.....	2
List of Figures.....	5
List of Tables .....	8
1. Executive Summary .....	9
2. Background .....	10
3. Research Objectives and Work Plan.....	14
4. Methodology.....	17
5. Results/Variations/Conclusions.....	19
5-1. Formation of Polyaluminum Hydrolysis Products	19
5-2. pH Dependent Model of Monoaluminum Hydrolysis Speciation and Aluminum Mineral Equilibria in the H-Al-Na-K-OH-Cl-H <sub>2</sub> O System to High Salt Concentration and Temperature.	21
5-2a. Parameterization of Al <sup>3+</sup> Interactions in the Low pH H-Al-Na-K-Cl-H <sub>2</sub> O System (0° to 100°C)	22
5-2b. Parameterization of the Standard Chemical Potentials of the Aqueous Al(OH) <sup>2+</sup> , Al(OH) <sub>2</sub> <sup>+</sup> , Al(OH) <sub>3</sub> <sup>0</sup> and Al(OH) <sub>4</sub> <sup>-</sup> Species (T: 0-300°C) and their Pitzer Interaction Parameters (T<100°C; 0-5 m NaCl) in the Intermediate pH Region	24
5-2c. Parameterization of the Al(OH) <sub>4</sub> <sup>-</sup> Aqueous Species Interactions and the Gibbs Free Energies of Reaction for the Minerals, Gibbsite and Boehmite, in the High pH Region (0-300°C)	24
5-2d. Final pH Dependent Model to High Temperature and to High NaCl Concentration	26
5-2e. Potassium Interactions in the H <sup>+</sup> -K <sup>+</sup> -Na <sup>+</sup> -Cl <sup>-</sup> -OH <sup>-</sup> -Al <sup>3+</sup> -Al(OH) <sup>2+</sup> -Al(OH) <sub>2</sub> <sup>+</sup> -Al(OH) <sub>3</sub> -Al(OH) <sub>4</sub> <sup>-</sup> -H <sub>2</sub> O System (0° to ≈100°C)	27
5-2f. Summary: A Predictive pH Dependent Model of Solution-Solid Equilibria in the H <sup>+</sup> -K <sup>+</sup> -Na <sup>+</sup> -Cl <sup>-</sup> -OH <sup>-</sup> -Al <sup>3+</sup> -Al(OH) <sup>2+</sup> -Al(OH) <sub>2</sub> <sup>+</sup> -Al(OH) <sub>3</sub> -Al(OH) <sub>4</sub> <sup>-</sup> -H <sub>2</sub> O(l) System to High Salt Concentration and Temperature:	28

<b>5-3. Model of Silica Aqueous Chemistry and Silica Solid Phases</b>	<b>29</b>
<b>5-4 Addition of Aluminosilicate Solid Phases to Model</b>	<b>31</b>
<b>5-5. Progress Developing an Isothermal 25°C Model of the Aluminum Sulfate in the H-Na-K-Al-Cl-H<sub>2</sub>O System.</b>	<b>38</b>
<b>6. References.....</b>	<b>40</b>
<b>7. Status DOE Supported Pitzer Model Development.....</b>	<b>43</b>
<b>8. Technology Transfer.....</b>	<b>44</b>
<b>9. DOE Related Publications .....</b>	<b>45</b>
<b>10. UCSD Team Members.....</b>	<b>48</b>

## LIST OF FIGURES

FIGURE	PAGE
<b>Figures 1-3:</b> Comparison of Pitzer and extended Debye Hückel model predictions of mineral solubility.	19
<b>Figure 4abc:</b> Effective equilibrium model predictions testing importance of polyaluminum oxohydroxo species. Percentage of aluminum in solution vs. pH at 25°C: (a) total aluminum concentration = .05 <i>m</i> . (b) total aluminum concentration = .01 <i>m</i> . (c) total aluminum concentration = .0075 <i>m</i> .	20
<b>Figure 5:</b> Effective equilibrium model predictions testing importance of polyaluminum oxohydroxo species. Percentage of aluminum in solution vs. pH at 100°C and total aluminum concentration = .035 <i>m</i> .	20
<b>Figure 6ab</b> Comparison of the low pH H-Al <sup>3+</sup> -K-Cl-H <sub>2</sub> O model (solid lines) and experimental solubility (symbols) in the AlCl <sub>3</sub> -KCl-H <sub>2</sub> O system at 0°, 25°, 40° and 80°C.	23
<b>Figure 7:</b> A comparison of the acid aluminum model calculations (solid lines) and experimental (symbols) sylvite and AlCl <sub>3</sub> .6H <sub>2</sub> O(s) saturation fields in the HCl-KCl-AlCl <sub>3</sub> -H <sub>2</sub> O system at 0°C, 25°C, and 80°C.	23
<b>Figure 8:</b> A comparison of the acid aluminum model calculations (solid lines) of the Al <sup>3+</sup> concentration in solutions in equilibrium with gibbsite as a function of pH (pH = -log [H <sup>+</sup> ]) at 30°, 50° and 70°C and I (NaCl) = 5 <i>m</i> with the experimental Al <sup>3+</sup> vs. pH data.	23
<b>Figure 9:</b> Comparison of model predicted molal concentrations ( <i>m</i> = mol.kg <sup>-1</sup> ) of the monoaluminum hydrolysis Al(OH) <sub>n</sub> species (light straight lines) in solutions in equilibrium with gibbsite as a function of pH (pH = -log [H <sup>+</sup> ]) at 50°C and I (NaCl) = 0.1 <i>m</i> with experiment	25
<b>Figure10:</b> Comparison of model predictions of the NaAl(OH) <sub>4</sub> concentration ( <i>m</i> = mol.kg <sup>-1</sup> ) in solutions in equilibrium with gibbsite as a function of NaOH concentration at 24.85°, 50° and 70.02°C with experiment.	25

<p><b>Figures 11, 12:</b> Model predictions (dashed lines) of the concentrations of <math>\text{Al}(\text{OH})_n^{3-x-y}</math> species and of total aluminum in .03 <i>m</i> NaCl solutions in equilibrium with boehmite as a function of pH (<math>\text{pH} = -\log [\text{H}]</math>). Fig. 11: <math>T \approx 200^\circ\text{C}</math> and Fig. 12: <math>T \approx 300^\circ\text{C}</math>. Symbols are the data.</p>	26
<p><b>Figure 13, 14:</b> Model predictions of <math>\text{Al}(\text{OH})_n</math> species concentrations (dashed straight lines) in solutions (Fig. 13: 1 <i>m</i> NaCl; Fig. 14: 5 <i>m</i> NaCl) in equilibrium with boehmite vs. pH (<math>\text{pH} = -\log [\text{H}^+]</math>) at <math>T \approx 150.0^\circ\text{C}</math>. Solid lines are the model prediction of the total aluminium concentration and symbols are data</p>	27
<p><b>Figure 15ab:</b> Comparison of model prediction of gibbsite solubility in NaOH-<math>\text{Al}(\text{OH})_4</math>-<math>\text{H}_2\text{O}</math> and KOH-<math>\text{Al}(\text{OH})_4</math>-<math>\text{H}_2\text{O}</math> solutions at <math>24^\circ</math>, <math>50^\circ</math> and <math>25^\circ\text{C}</math> with data.</p>	28
<p><b>Figure 16ab:</b> Model predictions of the distribution of species: <math>\text{Al}^{3+}</math>, <math>\text{Al}(\text{OH})^{2+}</math>, <math>\text{Al}(\text{OH})_2^+</math>, <math>\text{Al}(\text{OH})_3</math> and <math>\text{Al}(\text{OH})_4^-</math> as a function of pH at <math>90^\circ</math> and <math>300^\circ\text{C}</math>.</p>	29
<p><b>Figure 17:</b> Comparison of model predictions of the solubility of cristobalite in pure water as a function of temperature with experiment.</p>	30
<p><b>Figure 18:</b> Comparison of model predictions of the solubility of chalcedony in pure water as a function of temperature with experiment.</p>	30
<p><b>Figure 19:</b> Comparison of model kaolinite dissociation constants in alkaline solutions (<math>K_{s4}</math>; see Eq. 18) with <math>K_{s4}</math> values reported in the literature from <math>25^\circ\text{C}</math> to <math>250^\circ\text{C}</math>.</p>	30
<p><b>Figure 20:</b> Comparison of the model prediction of kaolinite solubility at high pH (<math>\text{pH} \approx 7-9</math>) and experiment) at <math>90^\circ\text{C}</math>. Also shown is the model prediction of dickite solubility.</p>	33
<p><b>Figure 21:</b> Model prediction of dickite solubility (total silicate concentration: <math>\sum m(\text{Si}) = m(\text{H}_4\text{SiO}_4^0) + m(\text{H}_3\text{SiO}_4^-)</math>) vs. pH at <math>25^\circ\text{C}</math> using standard free energy data (<math>\Delta_f G^0 m(298 \text{ K}, \text{ dickite})</math>) from Zotov et al. (1998) (solid line) and from Fialips et al. (2003) (dashed line). The predicted kaolinite solubility is also shown.</p>	33
<p><b>Figure 22:</b> Comparison of calculated total silica concentration (<math>\sum m(\text{Si}) = m(\text{H}_4\text{SiO}_4^0) + m(\text{H}_3\text{SiO}_4^+)</math>) of infinitely dilute solutions in equilibrium with kaolinite (lines) as a function of pH (<math>\text{pH} = -\log a_{\text{H}^+}</math>) and temperature (<math>25^\circ\text{C} - 200^\circ\text{C}</math>) with experimental kaolinite solubility data..</p>	33

<b>Figure 23:</b> The predicted solubility of the potassium feldspar, sanidine, in solutions containing the sodium feldspar, high-albite at 100°C.	33
<b>Figure 24:</b> The predicted dissolved aluminum concentration at the invariant points of the low (low-albite/microcline) and high (high-albite/sanidine) plagioclases at 100°C in a solution initially containing only NaCl,	35
<b>Figure 25</b> The model predicted solubility diagram for the system SiO <sub>2</sub> , low-albite, microcline, H <sub>2</sub> O at 100°C.	35
<b>Figure 26:</b> The model predicted solubility of kaolinite and quartz in pure water as function of pH.at 25°C and 150°C and comparison of the composition of the kaolinite-quartz coexistence point at these temperatures.	36
<b>Figure 27:</b> The model predicted stability fields of feldspar minerals, low series plagioclases (low-albite and microcline), in the ternary system NaAlSi <sub>3</sub> O <sub>8</sub> -KaAlSi <sub>3</sub> O <sub>8</sub> - H <sub>2</sub> O at 100°C. Composition of binary solutions MeAlSi <sub>3</sub> O <sub>8</sub> -H <sub>2</sub> O is also given.	36
<b>Figure 28:</b> The model predicted stability fields of feldspar minerals, high series plagioclases (high-albite and sanidine) in the ternary system NaAlSi <sub>3</sub> O <sub>8</sub> -KaAlSi <sub>3</sub> O <sub>8</sub> - H <sub>2</sub> O at 100°C. Composition of binary solutions MeAlSi <sub>3</sub> O <sub>8</sub> -H <sub>2</sub> O is also given.	36
<b>Figure 29:</b> Model prediction of the composition of sodium feldspar-potassium feldspars coexistence points as function of sodium chloride molality at 100°C.	36
<b>Figure 30:</b> Model prediction of the composition of sodium feldspar-potassium feldspars coexistence points as function of pH at 100°C.	37
<b>Figure 31:</b> Calculated composition (as Al <sub>total</sub> vs. Si <sub>total</sub> ) of solutions saturated with kaolinite at 110°C and constant pH (pH ≈ 8).	37
<b>Figure 32:</b> Calculated composition of (kaolinite + boehmite) coexistence point at 110°C as function of Al <sub>total</sub> and pH of solutions.	37
<b>Figure 33:</b> Comparison of model predictions with the observed solubilities in the Al <sub>2</sub> (SO <sub>4</sub> ) <sub>3</sub> .-Na <sub>2</sub> SO <sub>4</sub> -H <sub>2</sub> O ternary at 25°C.	37
<b>Figure 34:</b> Comparison of model predictions with the observed solubilities in the Al <sub>2</sub> (SO <sub>4</sub> ) <sub>3</sub> .-Na <sub>2</sub> SO <sub>4</sub> -H <sub>2</sub> O ternary at 25°C.	39
<b>Figure 35:</b> Comparison of model predictions with the observed solubilities in the Al <sub>2</sub> (SO <sub>4</sub> ) <sub>3</sub> .-K <sub>2</sub> SO <sub>4</sub> -H <sub>2</sub> O ternary at 25°C.	39

## LIST OF TABLES

<b>TABLE</b>	<b>PAGE</b>
<b>Table 1:</b> Research Work Plan, including go/no-go points	<b>16</b>
<b>Table 2:</b> Comparison of Pitzer model predictions of mineral solubility and predictions of extended Debye Hückel models.	<b>19</b>
<b>Table 3:</b> Minerals in the $H^+$ , $Na^+$ , $K^+$ , $Al^{3+}$ , $Cl^-$ , $Si(OH)_4$ , $SiO(OH)_3^-$ , $OH^-$ , $Al(OH)^{2+}$ , $Al(OH)_2^+$ , $Al(OH)_3^0$ , $Al(OH)_4^-$ , $H_2O$ system with standard free energy of reaction data	<b>32</b>
<b>Table 4:</b> Status DOE Supported Pitzer Model Development	<b>44</b>



## 1. EXECUTIVE SUMMARY

Successful exploitation of the vast amount of heat stored beneath the earth's surface in hydrothermal and fluid-limited, low permeability geothermal resources would greatly expand the Nation's domestic energy inventory and thereby promote a more secure energy supply, a stronger economy and a cleaner environment. However, a major factor limiting the expanded development of current hydrothermal resources as well as the production of enhanced geothermal systems (EGS) is insufficient knowledge about the chemical processes controlling subsurface fluid flow. Chemical interactions can have major effects on fluid flow in both hydrothermal and enhanced fluid limited reservoirs. For example, hydrothermal water or injected fluids that are out of equilibrium with rock formations can precipitate new mineral phases that alter or seal flow paths and drastically degrade the performance of the resource. An increased understanding and the ability to accurately predict the effect of subsurface fluid/rock chemical interactions on rock permeability and fluid flow with the accuracy needed would significantly optimize the economical production of geothermal energy. Unfortunately, characterizing these behaviors is difficult because they are complex functions of a system's composition (X), temperature (T) and pressure (P). Since these variables can change significantly over time, past experience and laboratory simulations may not be a reliable guide for future performance. Also, geochemical thermodynamic data in the literature often pertain to low temperatures (typically  $\approx 25^{\circ}\text{C}$ ) and/or to unrelated rock/water compositions.

With funding from past grants from the DOE geothermal program and other agencies, we successfully developed advanced equation of state (EOS) and simulation technologies that accurately describe the chemistry of geothermal reservoirs and energy production processes via their free energies for wide XTP ranges. The specific interaction equations of Pitzer (1973, 1987, 1991) can provide a very accurate description of the free energy of highly complex aqueous systems in the subcritical region to high concentration. Using these equations, we showed that our TEQUIL chemical models can correctly simulate behavior (e.g., mineral scaling and saturation ratios, gas break out, brine mixing effects, down hole temperatures and fluid chemical composition, spent brine incompatibilities) within the compositional range (Na-K-Ca-Cl-SO<sub>4</sub>-CO<sub>3</sub>-H<sub>2</sub>O-SiO<sub>2</sub>-CO<sub>2</sub>(g)) and temperature range (T < 300°C) associated with many current geothermal energy production sites that produce brines with temperatures below the critical point of water.

To treat higher temperature and pressure fluids in the supercritical region and problems requiring density variation, we developed other EOS phenomenologies and demonstrated, in more limited compositional ranges, that these models can also predict the chemistry of future very high P-T deep heat resources that are currently difficult to explore with traditional experimental methods. To transfer our technology, we also implemented an interactive web site ([geotherm.ucsd.edu](http://geotherm.ucsd.edu)). Our model parameterizations have been incorporated in many model packages both in the United States and in other countries (e.g., TEQUIL, EQ3/6NR, PHREEQ, GMIN, REACT, FLOTRAN, FREEZCHEM, ESP, TUFFREACT, SCAPE2).

The goal of research carried out under DOE grant DE-FG36-04GO14300 (10/1/2004-12/31/2007) was to expand the compositional range of our Pitzer-based TEQUIL fluid/rock interaction models to include the important aluminum and silica interactions (T < 300°C). Aluminum is the third most abundant element in the earth's crust; and, as a constituent of

aluminosilicate minerals, it is found in two thirds of the minerals in the earth's crust (Casey, 2003; Stefansson and Arnorsson, 2000; Moore, 1972). The ability to accurately characterize effects of temperature, fluid mixing and interactions between major rock-forming minerals and hydrothermal and/or injected fluids is critical to predict important chemical behaviors affecting fluid flow, such as mineral precipitation/dissolution reactions.

We successfully achieved the project goal and objectives by demonstrating the ability of our modeling technology to correctly predict the complex pH dependent solution chemistry of the  $\text{Al}^{3+}$  cation and its hydrolysis species:  $\text{Al}(\text{OH})^{2+}$ ,  $\text{Al}(\text{OH})_2^+$ ,  $\text{Al}(\text{OH})_3^0$ , and  $\text{Al}(\text{OH})_4^-$  as well as the solubility of common aluminum hydroxide and aluminosilicate minerals in aqueous brines containing components (Na, K, Cl) commonly dominating hydrothermal fluids. In the sodium chloride system, where experimental data for model parameterization are most plentiful, the model extends to 300°C. Determining the stability fields of aluminum species that control the solubility of aluminum-containing minerals as a function of temperature and composition has been a major objective of research in hydrothermal chemistry.

Interactions of aluminum with potassium ( $T \leq 100^\circ\text{C}$ ) and sulfate ( $T = 25^\circ\text{C}$ ) under this grant are limited to lower temperatures due to lack of data for model parameterization. Publications resulting from research carried out during this grant as well as during previous Department of Energy grants are given in section 9. This work has also been presented at conferences.

Models of rock/water chemistry that include aluminum not only are necessary to optimize the economical expansion of geothermal energy production but they also have application to other important energy related problems (e.g., scaling prediction in petroleum production systems, stripping towers for mineral production processes, nuclear waste storage,  $\text{CO}_2$  sequestration strategies, global warming). In addition, they can be valuable tools to understand a wide variety of other important fluid/rock phenomena (e.g., weathering, porosity/permeability changes, mobilization of metal ions in fluids and soils, aluminium ore production) affecting the evolution of many natural waters, soils and mineral deposits.

## 2. BACKGROUND

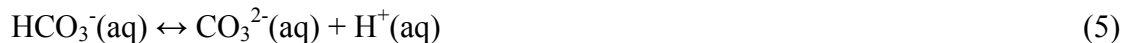
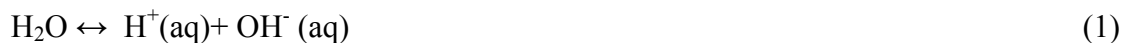
To significantly advance the use of geothermal energy, new technologies are needed to increase the understanding and facilitate the accurate prediction of resource chemical behaviors and production chemistry (DOE Specific Plan, 1998). Characterizing these behaviors is difficult because they are complex functions of a system's composition (X), temperature (T) and pressure (P). With funding from previous geothermal grants from the Department of Energy (e.g., DE-FG07-99ID13745) and from other agencies (e.g., DOE Basic Energy Sciences, the National Science Foundation and the Petroleum Research Fund), we have carried out research projects to develop computer based modeling technologies that can handle these complexities (see section 9). In the DOE geothermal program, we have shown that, with careful choice of methodology and parameterization, chemical equilibrium models based on thermodynamics and free energy descriptions can correctly simulate subcritical chemical behavior in the ranges of fluid compositions, formation minerals, temperature and pressure associated with many hydrothermal and enhanced geothermal systems as well as for the very high PT supercritical chemistry of deep resources that is

difficult to study with traditional experimental methods. Substantial progress has been made on two model packages.

The TEQUIL models incorporate the specific interaction equations of Pitzer (1973, 1987, 1991) and apply to subcritical geothermal operations ( $T < 300^{\circ}\text{C}$ ) where the major effect on the free energy of hydrothermal fluids is from changes in solute concentrations and temperature. These models can be used to interpret field chemistry measurements, predict resource and production chemical behavior (e.g., solute/solvent activities, mineral saturation ratios, mineral scaling, fluid mixing, flashing, scaling, pH effects), assess performance and test problem abatement strategies. For example, mineral precipitation (e.g., calcite or silicate scaling) can not only damage plant equipment and wells (Benoit, 1987; Harrar et al., 1982) but can also significantly decrease the permeability of the formations containing hydrothermal fluids or injectates. In constructing these models, we assess and extend the applicability of large amounts of experimental data in the literature. The GEOFLUIDS models incorporate EOS phenomenologies that treat multiple phase processes, such as flashing and miscibility, to high T, P supercritical conditions. We have demonstrated, in more limited compositional ranges that these models can predict the chemistry of very high P-T deep heat resources that is currently difficult to explore with traditional experimental methods.

To transfer our technology, we also implemented an interactive web site ([geotherm.ucsd.edu](http://geotherm.ucsd.edu)). To accomplish this, comprehensive user interfaces were developed. Several of the validated TEQUIL and GEOFLUIDS codes have been installed on this site which is accessed by users nationally and internationally. Publications resulting from these studies are listed in section 9. Our model parameterizations have been incorporated in many model packages both in the United States and in other countries (e.g., TEQUIL, EQ3/6NR, PHREEQ, GMIN, REACT, FLOTRAN, FREEZCHEM, ESP, TUFFREACT, SCAPE2).

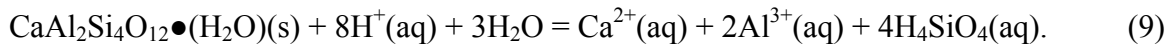
Prior to grant DE-FG36-04GO14300, our Pitzer-based TEQUIL models included interactions of the dominant brine components ( $\text{Na}^+$ ,  $\text{K}^+$ ,  $\text{Ca}^{2+}$ ,  $\text{Cl}^-$ , and  $\text{SO}_4^{2-}$ ),  $\text{CO}_2$  gas reactions, the scale-formers gypsum, calcite and silica and the acid-base solution equilibria shown in Eq's. 1-8.



The goal of the research project funded under DOE grant DE-FG36-04GO14300 (10/1/2004-12/31/2007) was to increase the applicability of our TEQUIL suite of models to understanding subsurface chemical processes affecting fluid flow in hydrothermal and

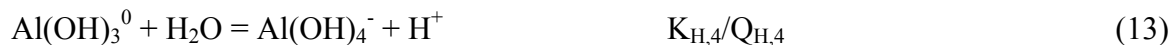
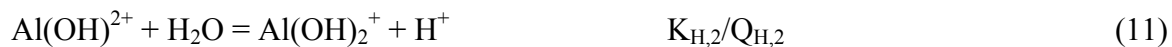
enhanced geothermal systems by expanding their fluid/rock compositional range to include aluminum interactions and equilibria with important aluminum hydroxide and aluminosilicate minerals. Aluminosilicates, which make up two thirds of the minerals in the earth's crust (Casey, 2003; Stefansson and Arnorsson, 2000; Moore, 1972), are found as feldspars (e.g., alkali feldspar, Na/KAlSi<sub>3</sub>O<sub>8</sub>) in metamorphic and igneous rock (Deer et al., 1966) as well as clays in well-weathered soils (Driscoll and Schecher, 1989) and as authigenic constituents of evaporates (Kastner, 1971).

In order to interpret the effects of injection or formation fluid interactions with aluminosilicate minerals, we need to be able to estimate the activities of all the species in their dissolution reactions. For example, the hydrothermal mineral, wairakite (CaAl<sub>2</sub>Si<sub>4</sub>O<sub>12</sub>•(H<sub>2</sub>O)), undergoes dissolution via the reaction shown in Eq. 9.



Consequently, accurate models of aluminum and silica aqueous chemistry form essential foundations for modeling aluminosilicate mineral solubilities (precipitation and dissolution reactions). Silica aqueous chemistry (Eq. 3) was successfully modeled with funding from our previous DOE grant (DE-FG07-99ID13745). Therefore a primary objective of DOE grant DE-FG36-04GO14300 (see section 3) was to demonstrate the ability of our Pitzer-based modeling technology to accurately predict the aqueous chemistry of aluminum as a function of pH and fluid concentration over a wide range of temperature for application to energy production from subcritical hydrothermal and enhanced geothermal systems.

The aqueous chemistry of aluminum is highly complicated. Polyaluminum species (e.g. Al<sub>2</sub>(OH)<sub>2</sub><sup>4+</sup>, Al<sub>3</sub>(OH)<sub>4</sub><sup>5+</sup>, Al<sub>13</sub>O<sub>4</sub>(OH)<sub>24</sub><sup>7+</sup> or Al<sub>13</sub>O<sub>4</sub>(OH)<sub>24</sub>(H<sub>2</sub>O)<sub>12</sub><sup>7+</sup>) have been proposed to explain data in concentrated aluminum solutions in certain pH ranges. However, there are insufficient data available to accurately model the interactions of these species. For sufficiently low concentration, the accepted aluminum hydrolysis reactions are given in Eq's 10-13 (K and Q are the equilibrium constant and concentration dependent equilibrium quotients, respectively).



The experimental data available for parameterizing the aqueous chemistry of the Al<sup>3+</sup> cation and the hydrolysis species, Al(OH)<sup>2+</sup>, Al(OH)<sub>2</sub><sup>+</sup>, Al(OH)<sub>3</sub><sup>0</sup>, and Al(OH)<sub>4</sub><sup>-</sup>, in the high and low pH region include osmotic, potentiometric and solubility measurements. In the near neutral pH region, most commonly encountered in natural systems, the low solubility and complex solution chemistry of aluminum have made the determination of the activity and formation constants of the various aluminum species difficult. However, recent advances in potentiometric titration methods and in determining effective formation constants for aluminum speciation reactions as a function of solution composition via solubility studies of

the aluminohydroxo minerals (e.g., gibbsite  $\text{Al}(\text{OH})_3(\text{cr})$ ; boehmite  $\text{AlOOH}(\text{cr})$ ) are now providing the data needed to characterize the thermodynamics of  $\text{Al}^{3+}$  and its monoaluminum hydrolysis products as a function of pH, including the important intermediate pH region.

The major limitations to achieving the research project goal were: (1) the complex nature of aluminum aqueous chemistry which includes multiple pH dependent species as well as possible polymeric aluminum species; (2) the poor availability of aluminum solution data in salt solutions, particularly above  $100^\circ\text{C}$ , for parameterizing the solution interactions of the various aluminum hydrolysis solutes; and, (3) the poor availability of solubility data for the aluminum minerals to directly calculate the free energies of reaction that are necessary to predict equilibrium with these minerals. However, following the work plan given in Table 1, we successfully overcame these limitations (see go/no-go points in Table 1) and achieved the project goal and objectives (see results in section 5).

To evaluate the importance of polyaluminum hydrolysis species, we developed an approximate model at  $25^\circ\text{C}$  and  $100^\circ\text{C}$  using the concentration products for  $\text{Al}^{3+}$  hydrolysis producing polyaluminum ion species taken from the studies of Baes and Mesmer (1986) and Furrer et al. (1992) (see section 5-1). Model predictions showed that an accurate pH dependent model of aluminum aqueous chemistry could be developed for application to a wide range of reservoir fluids in equilibrium with their surroundings using only monoaluminum hydrolysis products. This finding overcame one of the important go/no-go points in this project (see Table 1).

Using data for the sodium chloride system, we developed a model that correctly predicts the complex pH dependent solution chemistry of the  $\text{Al}^{3+}$  cation and its hydrolysis species:  $\text{Al}(\text{OH})^{2+}$ ,  $\text{Al}(\text{OH})_2^+$ ,  $\text{Al}(\text{OH})_3^0$ , and  $\text{Al}(\text{OH})_4^-$  to high solution concentration in the  $0^\circ - 300^\circ\text{C}$  temperature range (see sections 5-2a-d). The NaCl system was chosen because  $\text{Na}^+$  and  $\text{Cl}^-$  are major components of geothermal fluids, and it has the most experimental data for model parameterization and for testing model predictions to high temperature. The successful achievement of this objective overcame critical go/no-go points (see Table 1) in the project. Note that in this process, solubility prediction of the important aluminum hydroxide minerals, gibbsite ( $\text{Al}(\text{OH})_3$ ) and boehmite ( $\text{AlOOH}$ ), were added to the model. Interactions with potassium (see Table 1 and section 5-2e) were added but are limited to lower temperature ( $\approx 100^\circ\text{C}$ ) due to lack of data for model parameterization. Preliminary investigation of the aluminum sulfate system was initiated at  $25^\circ\text{C}$  (see section 5-5).

With the development of a model of aqueous aluminum chemistry in the H-Na-K-OH-Cl- $\text{Al}^{3+}$ - $\text{Al}(\text{OH})^{2+}$ - $\text{Al}(\text{OH})_2^+$ - $\text{Al}(\text{OH})_3^0$ - $\text{Al}(\text{OH})_4^-$ - $\text{H}_2\text{O}$  system (NaCl:  $0^\circ - 300^\circ\text{C}$ ; KCl:  $0^\circ - 100^\circ\text{C}$ ) under this grant (see above), our comprehensive suite of TEQUIL solution models includes many of the components necessary to describe the saturation status of hydrothermal fluids in contact with important aluminosilicate minerals (see those compiled in the report of Browne (BROWNE, 1978) for the temperature, pressure, and concentration (TPX) conditions encountered in many geothermal applications. Unfortunately, the availability of data for directly calculating the Gibbs free energy of aluminum silicate minerals is poor. Therefore we must rely on thermodynamic data bases available in the literature to calculate the free energy of reaction of most of these minerals.

Combining our new aluminum model and our updated TEQUIL silicate model (see section 5-3), we first added equilibria with several hydrothermal aluminosilicate minerals that have both free energy data and solubility data in the literature to test the feasibility of incorporating aluminosilicate mineral free energies in the literature in our model

to predict their solubilities (important go/no-go point; Table 1). Using just equilibrium constant data ( $\Delta G_{f,T}^0(m)$ ) in the literature to establish temperature functions for the free energy of reaction of these aluminosilicate minerals (e.g., kaolinite and dickite ( $\text{Al}_2\text{Si}_2\text{O}_5(\text{OH})_4(\text{cr})$ ), we showed that our model calculations are in good agreement with their complicated pH dependent solubility data available from 25° to 250°C. We also showed that using only infinite dilution equilibrium constant data determined in a specific pH region we could successfully predict very complicated solubility behavior over a very wide pH range from low to high temperature.

Sodium and potassium feldspars and pure silica minerals are some of the most common hydrothermal formation minerals. We successfully added (see sections 5-3 and 5-4) amorphous silica ( $\text{SiO}_2 \cdot 2\text{H}_2\text{O}$ ), the pure silica ( $\text{SiO}_2$  (cr)) polymorphs: quartz, chalcedony and cristobalite as well as the Na- and K-Al-Si minerals (sodium feldspars (low-albite and high-albite) and potassium feldspars (microcline, a low series feldspar, and sanidine, a high series feldspar). The good agreement with the Arnorsson and Stefansson (1999) equilibrium constant data for Na, aluminosilicates to 300°C and for K aluminosilicates to 100°C showed that our aluminum and silicate solution models are compatible with this very important comprehensive aluminosilicate thermodynamic data base to high temperature, overcoming important research go/no-go points (see Table 1): (1) the compatibility of our silica and aluminum solution models; (2) the compatibility of these models and mineral equilibrium constants in the literature.

The results given in section 5 show that by focusing principally on aluminum interactions in NaCl solutions, which have most of the aluminum activity and hydrolysis speciation data and aluminum mineral solubility data, limitations to achieving project goals and objectives were overcome. Therefore this project allowed us to develop and validate the methods necessary to include many other solids in this extremely important class of rock-forming minerals. We believe that our research results achieved important milestones: (1) the construction of the first model, tailored to high solution concentration mixing behavior, that accurately describes aluminum aqueous chemistry from low to high pH in the H-Na-K-OH-Cl-Al<sup>3+</sup>-Al(OH)<sup>2+</sup>-Al(OH)<sub>2</sub><sup>+</sup>-Al(OH)<sub>3</sub><sup>0</sup>-Al(OH)<sub>4</sub><sup>-</sup>-H<sub>2</sub>O system to high temperature (NaCl:~0°-300°C; KCl:~0°-100°C). (2) the addition of silica and aluminosilicate solubility prediction to this model

This work has been transferred via conferences and publications. Section 9 lists publications resulting from research carried out during this grant as well as during previous Department of Energy grants. To transfer our technology we also developed an interactive web site (geotherm.ucsd.edu) with funding from previous DOE geothermal grants. Several validated models have been installed on this web site in the past but funding has not been available to update this web site (user codes, user documentation and new validated models).

### **3. RESEARCH OBJECTIVES AND WORK PLAN**

#### **3-1 RESEARCH OBJECTIVES/RELEVANCE**

To optimize the production of energy from hydrothermal and enhanced geothermal systems, the current understanding of the subsurface rock-water chemical processes controlling fluid flow must be significantly improved. Because of the great abundance of

aluminum hydroxide and aluminosilicate minerals in a wide range of rock types throughout the earth's crust, our research objective with funding from DOE grant DE-FG36-04GO14300 was to expand our suite of Pitzer-based chemical modeling technologies to include aluminum aqueous chemistry and equilibrium dissolution and precipitation reactions with these major rock-forming minerals in the composition, temperature and pressure ranges important to many geothermal energy R&D and energy production operations. Such comprehensive models are currently not available. To achieve this goal we proposed to construct high accuracy models that can cost effectively and accurately interpret field chemistry measurements, predict resource and production system chemical behavior (e.g., predict mineral saturation ratios and scaling, effects of fluid mixing, flashing, fluid mixing on mineral precipitation/dissolution and thereby on formation permeability and fluid circulation) as a function of temperature, composition, and pH. These models will provide a means to rapidly identify chemical problems in production wells and power plants, facilitate the accurate analysis of the performance of the hydrothermal resource and provide a means to assess the effects of abatement strategies such as chemical treatments, hydrofracturing and fluid injection. To successfully develop such a model we proposed to collect and validate large amounts of thermochemical data of aluminum aqueous chemistry and aluminum mineral solubility that are useful for exploration and development of geothermal resources as well as identify areas where more laboratory measurements are especially needed for application to geothermal problems. In addition, our objective was to transfer and data evaluation to the geothermal community and other researchers via publications, workshops and our interactive web site, [geotherm.ucsd.edu](http://geotherm.ucsd.edu). This modeling research has broader impacts in other energy related areas (e.g., scaling prediction in petroleum production systems, stripping towers for mineral production processes, nuclear waste storage, CO<sub>2</sub> sequestration strategies, global warming). They provide valuable tools to help understand a wide variety of other important fluid/rock phenomena (e.g., weathering, porosity/permeability changes, mobilization of metal ions in fluids and soils, aluminum ore production) affecting the evolution of many natural waters, soils and mineral deposits. They can be used to help train experts in the geothermal industry, chemical modeling and earth science

### **3-2. SPECIFIC TECHNICAL OBJECTIVES**

To achieve the project goals, technical objectives of this program (see Tasks in Table 1) were to:

- Collect and assess thermodynamic data in the literature available for parameterizing a model of aluminum aqueous chemistry and aluminum mineral solubility in the 25°C-300°C temperature range.
- Assess the temperature, pH and concentrations ranges where the contribution of polymeric aluminum species, which have very poor data availability, can be neglected.
- Develop an accurate pH dependent model of aluminum hydrolysis speciation and aqueous interactions and aluminum hydroxide mineral solubility in the sodium chloride system, where experimental data are most available, to 300°C and to high solution concentration using the Pitzer formalism.
- Add potassium interactions as data allow.
- Integrate our aluminum model and our model of silica aqueous chemistry and silica solubility.
- Collect and assess thermodynamic data in the literature available for adding solubility predictions of Na/Kaluminosilicate minerals to this model.
- Assess the data

available in the literature for parameterizing aqueous aluminum-sulfate interactions and construct a model within a limited temperature and concentration range.

### 3-3 RESEARCH WORK PLAN AND GO/NO-GO POINTS

**TABLE 1: Grant Research Work Plan**

TASKS	GO/NO-GO POINTS
1. Test if polymeric Al hydrolysis complexes can be neglected in EGS applications.	Ability to construct a useful chemical model that does not require the addition of polymeric Al hydrolysis species, which have poor data availability.
2. Assess available activity, solubility and Al hydrolysis equilibrium constants data for the Al speciation scheme, $\text{Al}^{3+}$ , $\text{Al}(\text{OH})^{2+}$ , $\text{Al}(\text{OH})_2^+$ , $\text{Al}(\text{OH})_3$ and $\text{Al}(\text{OH})_4^-$ required to make a pH dependent aqueous Al chemistry model that extends from low temperature to $\approx 300^\circ\text{C}$ . in NaCl solutions ( $I_{\text{max}} = 5\text{ m}$ ).	Availability and quality of data suitable for model construction.
3. Use activity, solubility and Al hydrolysis speciation constant data to make a pH dependent model of Al chemistry based on the monoaluminum speciation of task 2. to to $\approx 300^\circ\text{C}$ in NaCl solutions ( $I_{\text{max}} = 5\text{ m}$ ).	Compatibility of activity data and Al hydrolysis species equilibrium constant data. Compatibility of equilibrium constants and our sodium acid/base solution model. Ability to extrapolate some temperature functions for Al interaction model parameters established in different temperature regions and correctly reproduce the complicated Al chemistry in NaCl aqueous solutions.
4. Add equilibria with aluminum hydroxide and sodium-aluminum-silicate minerals for which solubility data are available in the literature to test feasibility of approach in task 6..	Availability and quality of solubility data. Compatibility of our silica solution and aluminum solution models. Compatibility of Al solution model and solubility data/ mineral free energy data in the literature as a function of pH, temperature and solution composition.
5. Repeat above steps for potassium/Al solutions and minerals.	Similar points as with the Na/Al system but with the additional difficulty that there are fewer data for KCl solutions.
6. Using thermodynamic data bases in the literature to add equilibria with Na-K-Al-Si minerals for which only free energy of reaction data is available from data bases.	Compatibility of these literature data bases and our model.
7. Begin developing a low temperature model of aluminum-sulfate interactions as time allows.	Very limited availability of solution data.



## 4. METHODOLOGY

### TEQUIL, Free Energy Models to Temperatures near 300°C

The temperatures of the hydrothermal systems accessed by present day geothermal systems and those projected in the near future are below the critical point of pure water. In this situation the fluids are nearly incompressible and the largest variation in the solution free energy comes from changes in solute composition and temperature. Successful equation of state (EOS) models for these subcritical systems must be able to accurately describe changes in the dissociation state of solutes as well as efficiently treat important mixing effects and solid-liquid-gas equilibria to high fluid concentration as a function of temperature.

The specific interaction equations of Pitzer (1973, 1987, 1991) can provide a very accurate description of the free energy of highly complex aqueous systems in the subcritical region to high concentration. Although the Pitzer equations are based on theory, they contain parameters that must be evaluated. However, since the equations expand the excess Gibbs free energy of the solution phase to third virial coefficient terms in composition, only binary and ternary system data are necessary for full parameterization of a model for complicated, multicomponent systems. In the model discussed here our (Harvie and Weare, 1980; Harvie, Moller and Weare, 1984; Weare, 1987, Moller 1988) implementation of the Pitzer activity expressions for the aqueous solution phase is used. These equations have been presented in many publications (e.g., Pitzer, 1987; Pizer 1991; Harvie, Moller and Weare, 1984; Moller, 1988) and are included below for reference. An ideal mixture or mixing equation of state is used for the vapor phase and the solid phases are assumed to be pure.

In Eq. 14 we give the model expression for the activity coefficient of a cation, M, that is based on interactions of M with the other solute species in the fluid. In this expression  $m$  is  $mol.kg^{-1}$ .

$$\begin{aligned} \ln \gamma_M &= z_M^2 F + \sum_a m_a (2B_{Ma} + ZC_{Ma}) + \sum_c m_c (2\Phi_{Mc} + \sum_a m_a \psi_{Mca}) + \sum_{a < a'} \sum m_a m_{a'} \psi_{Maa'} + |z_M| \sum_c \sum_a m_c m_a C_{ca} \\ &\quad + \sum_n m_n (2\lambda_{nM}) + \sum_n \sum_a m_n m_a \zeta_{naM} \\ F &= -A^\phi \{ I^{.5} / (1 + 1.2I^{.5}) + (2/1.2) \ln(1 + 1.2I^{.5}) \} + \sum_c \sum_a m_c m_a B'_{ca} + \sum_c \sum_{c' < c} m_c m_{c'} \Phi'_{cc'} + \sum_a \sum_{a' < a} m_a m_{a'} \Phi'_{a'a} \\ B_{ma} &= \beta_{Ma}^0 + \beta_{Ma}^1 g(\alpha, I^{.5}) + \beta_{Ma}^2 g(12I^{.5}), \quad g(x) = 2(1 - (1+x)e^{-x})/x^2, \quad \Phi_{ij} = \Theta_{ij} + {}^E \Theta_{ij}(I), \quad Z = \sum_i |z_i| m_i \end{aligned} \quad (14)$$

This expression is symmetric for an anion. The  $B$  coefficients describe the ionic strength dependence of binary solutions. When either the cation or anion for an electrolyte is univalent, we set  $\alpha$  equal to 2.0 and omit the  $\beta^{(2)}$  term. For 2-2 or higher valence pairs,  $\alpha = 1.4$ . The  $\beta^{(2)}$  term accounts for the increased tendency of higher charged species to associate in solution. The ionic strength dependence of the ternary mixing coefficients is found in the  $\Phi$  terms, which account for mixing between two ions of like charges. In  $\Phi_{ij}$ ,  $\Theta_{ij}$  is the only adjustable parameter. The ionic strength dependent  ${}^E \Theta_{ij}(I)$  term accounts for electrostatic

unsymmetric mixing effects that depend only on the charges of ions  $i$  and  $j$  and the total ionic strength. In this model the third virial coefficients,  $C$ , and the  $\psi$  terms, are independent of ionic strength. In Eq. 14, the terms with  $\lambda$  and  $\zeta$  account for neutral species interactions with anions and cations (Felmy and Weare, 1986) Equation 15 below shows the expression for the activity coefficient of a neutral species such as  $\text{Al}(\text{OH})_3^0$ .

$$\ln \gamma_N = \sum_c m_c (2\lambda_{N,c}) + \sum_a m_a (2\lambda_{N,a}) + \sum_c \sum_a m_c m_a \zeta_{N,c,a} \quad (15)$$

Temperature dependence (e.g., Moller, 1988; Greenberg and Moller, 1989) of the solution parameters is built into the model by adjusting selected constants in the following equation,

$$\text{Parameter (T)} = a_1 + a_2 T + a_3 (T^2) + a_4 (T^3) + a_5 / T + a_6 \ln T + a_7 (1/(T-263)) + a_8 (1/(680-T)). \quad (16)$$

All these parameters are adjusted to fit the available data in binary and ternary systems where possible using a non-linear least squares method (Harvie, 1987). We note that only binary and ternary data are required to evaluate all the parameters in the Pitzer equations described here no matter how many components are in the solution. Eqs. 14-16, therefore, provide a means to extrapolate data from ternary and lower systems to systems of higher order. Parameters established in one system can also be transferred to different systems. We have shown that these equations can provide solubility predictions for a range of ionic strengths that include most of the compositions found in nature.

To constrain our parameter evaluation as much as possible in our modeling program we include all measurements available in our data base. This, for example, means that data for very low and high pH values, which not usually encountered in natural waters, are used to evaluate the parameters in the aqueous aluminum system. Due to the strong hydrolysis in this system the  $\text{Al}^{3+}$  ion dominates the aluminum solute species concentrations only at low pH; therefore this is the region where measured thermodynamic properties are most sensitive to  $\text{Al}^{3+}$  parameters (e.g.  $\beta_{al,Cl}^{0,1}$  and  $\theta_{Al,H}$  in Eq. 14). This focus on including all the data not only generalizes the model to treat very low and high pH hydrothermal brines but also allows the evaluation of parameters in composition regions where they make the largest and most independent contribution, thereby increasing the reliability of the model.

Using these equations and our solubility modeling approach, we have shown (e.g., see Fig's 1-4) that chemical models can be developed that accurately predict complicated solid-liquid-vapor equilibria in complex multicomponent systems to high solution concentration and temperature (e.g., see Harvie, Moller, Weare (HMW), 1984; Moller, 1988; Greenberg and Moller, 1989; Moller et al., 1998; Christov and Moller, 2004ab; Christov, Dickson, Moller, 2007). Figures 1 and 2 compare predictions of gypsum/anhydrite scale solubility using extended Debye-Huckel models (indicated by "B-Dot" or EQ3/6) and our TEQUIL Pitzer-based models (Fig's. 1, line marked HMW; Fig. 2, solid lines) with experimental data (symbols) at 25°C and 100°C. In Fig. 3 (from Bethke, 1996) B-dot predictions (D-H) of

halite and anhydrite saturation are compared with those of the TEQUIL model (HMW) and those of Pitzer at 25°C in higher ionic strength brines ( $I \approx 6 m$ ). These brines, which are in equilibrium with solid halite and anhydrite, should have saturation indices of 1. In Table 2, we compare the saturation ratios (at 25°C) calculated from the B-dot model (Bethke, 1996) with those of our TEQUIL model (see Reed, 1989). It is well known that seawater ( $I = 0.719m$ ) is supersaturated with respect to the calcium carbonate. This behavior is accurately predicted by the TEQUIL model.

**Figure 1**

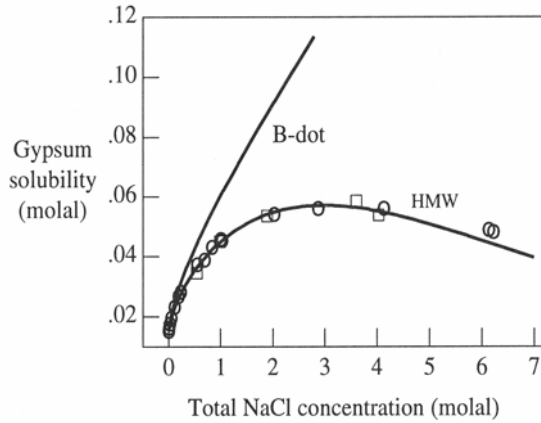


**Figure 2**

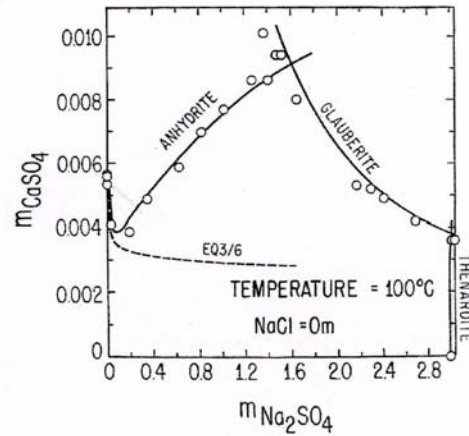


**Figure 3**

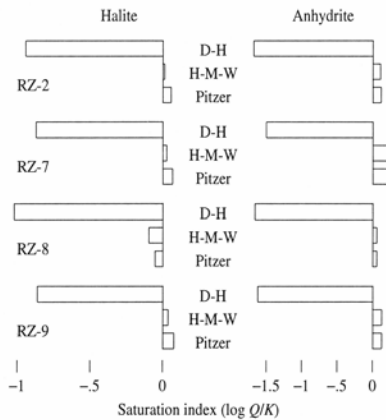


**Table 2**

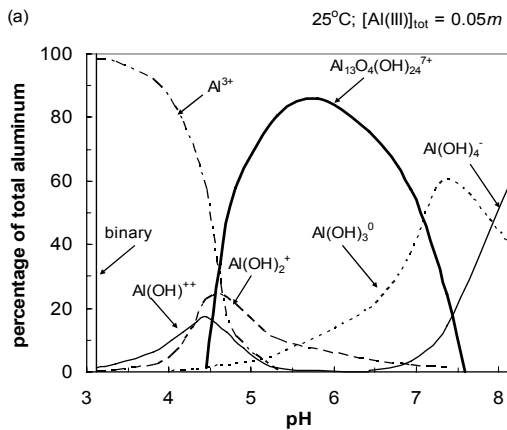
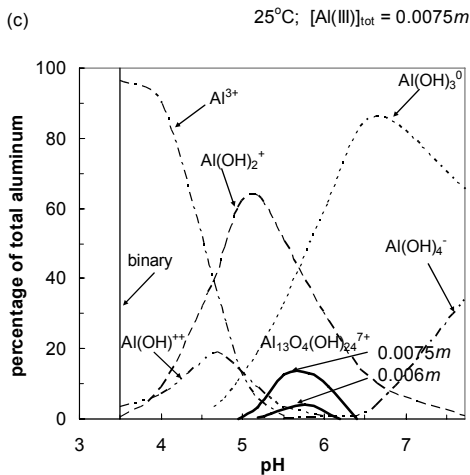
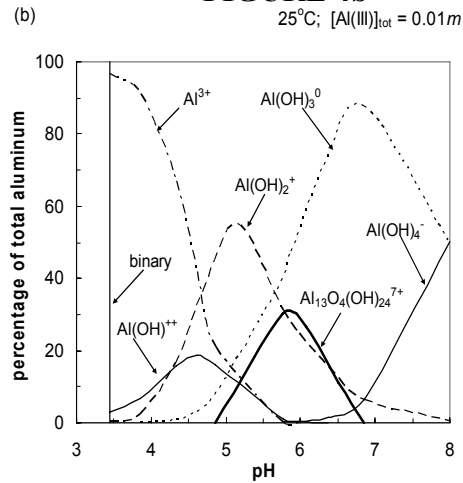
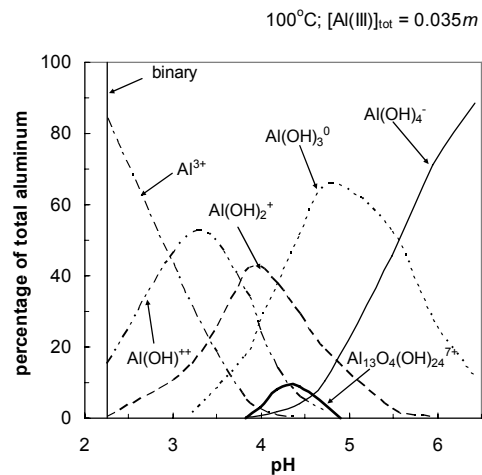
SATURATION OF CARBONATE SCALING MINERALS		
In Seawater ( $I = 0.719m$ )		
	TEQUIL	B-Dot (Bethke)
Calcite	6.86	0.81
Aragonite	4.88	0.64
In Dixie Valley Brine (0.014m) (Reed)		
Calcite	0.667	0.611

## 5. RESULTS/ VARIANCES/CONCLUSIONS

### 5-1. FORMATION OF POLYALUMINUM OXO-HYDROXO HYDROLYSIS SPECIES

Polyaluminum oxo-hydroxo species (e.g.  $Al_2(OH)_2^{4+}$ ,  $Al_3(OH)_4^{5+}$ ,  $Al_{13}O_4(OH)_{24}^{7+}$  or  $Al_{13}O_4(OH)_{24}(H_2O)_{12}^{7+}$ ) have been proposed to explain data in concentrated aluminum

solutions in certain pH ranges. To test the importance of these species in waters with higher concentrations of aluminum, we developed an approximate model at 25°C and 100°C using the concentration products for  $\text{Al}^{3+}$  hydrolysis species ( $\text{Al}^{3+}$ - $\text{Al}(\text{OH})^{2+}$ - $\text{Al}(\text{OH})_2^+$ - $\text{Al}(\text{OH})_3^0$ - $\text{Al}(\text{OH})_4^-$ ) and aluminum polymetal reactions taken from the studies of Baes and Mesmer (1986) and Furrer et al. (1992). Using this model, we examined the importance of polyaluminum oxo-hydroxo species in various total aluminum concentration, pH and temperature ranges. Examples of predictions at 25°C, where the model is best defined, are shown in Fig's. 4abc. Figure 5 shows results at 100°C. In these figures the pH of a binary  $\text{AlCl}_3$ - $\text{H}_2\text{O}$  solution is indicated by the line marked "binary."

**FIGURE 4a****FIGURE 4c****FIGURE 4b****FIGURE 5**

Model predictions (Fig's. 4a-c) show that the only polyaluminum species that appears in significant concentration is  $\text{Al}_{13}\text{O}_4(\text{OH})_{24}^{7+}$ . There is good evidence that this species exists in metastable concentrated aluminum solutions. Our calculations showed that this species is

important in the intermediate pH range ( $\approx 4-8$ ) in solutions with total aluminum concentrations above approximately 0.001 *m*. In highly acidic waters the low OH concentration destabilizes the formation of polyaluminum species and  $\text{Al}^{3+}$  predominates although the concentration of aluminum can be high. In very high pH waters with higher aluminum concentration, the dominant aluminum species is the noncondensable hydrolysis product,  $\text{Al}(\text{OH})_4^-$  (see Eq. 13).

The appearance of the  $\text{Al}_{13}\text{O}_4(\text{OH})_{24}^{7+}$  species in the intermediate pH range was a concern because most natural waters fall in the intermediate pH range. However, model calculations showed that as the total aluminum concentration decreases, the concentration of the  $\text{Al}_{13}\text{O}_4(\text{OH})_{24}^{7+}$  species in the intermediate pH range falls dramatically. For example, the model predicts that the concentration of this species is less than 9% for a total aluminum concentration of 0.006 *m* (see solid line in the 5-6 pH range in Fig. 4c). At higher temperature, this highly charged species is even less stable. Most natural waters, which typically fall in the intermediate pH range, have much lower total aluminum concentrations (e.g.,  $m_{\text{Al}} < 10^{-5}$ ), reflecting equilibrium with low solubility aluminum hydroxy minerals, such as gibbsite ( $\text{Al}(\text{OH})_3$ ) and kaolinite ( $\text{Al}_2\text{Si}_2\text{O}_5(\text{OH})_4$ ), that are common to most formations and soils. Therefore, assuming that the equilibrium constants we used in constructing our model provide at least qualitatively correct behavior, our calculations suggested that an accurate pH dependent model of aluminum aqueous chemistry could be developed for application to a wide range of reservoir fluids in equilibrium with their surroundings using only monoaluminum hydrolysis products. This finding overcame one of the important go/no-go points in this project (see Table 1).

## **5-2. pH DEPENDENT MODEL OF MONOALUMINUM HYDROLYSIS SPECIATION AND ALUMINUM MINERAL EQUILIBRIA IN THE H-Al-Na-K-OH-Cl-H<sub>2</sub>O SYSTEM TO HIGH SALT CONCENTRATION AND TEMPERATURE**

This section describes the construction of a Pitzer interaction model that calculates aluminum aqueous chemistry based on the species:  $\text{Al}^{3+}$ ,  $\text{Al}(\text{OH})^{2+}$ ,  $\text{Al}(\text{OH})_2^+$ ,  $\text{Al}(\text{OH})_3^0$ ,  $\text{Al}(\text{OH})_4^-$  in H-Al-Na-K-OH-Cl-H<sub>2</sub>O solutions as a function of pH to high salt concentration (5 *m*) and high temperature. In the sodium chloride system, where experimental data for model parameterization are most plentiful, the model extends to 300°C. Interactions with potassium are limited to lower temperature (100°C) due to lack of data for model parameterization.

At fixed temperature, the stability fields of  $\text{Al}^{3+}$  and its hydrolysis species, which control the solubility of aluminum containing minerals, change as the solution pH changes. Determining these fields as a function of temperature and composition is a major objective of research in hydrothermal chemistry and of the research in this program. Parameterization of the aluminum species interactions with other solute species requires the evaluation of a very large number of parameters (see Pitzer equations in section 4). The data base for determining these parameters is not extensive. However, a very significant advantage of the Pitzer mixing theory is the transfer of common parameter between systems. This means that parameters that have been accurately determined in systems with more complete data bases can be transferred to less well defined systems. For this model, the temperature functions for the water chemical potential, and for the Debye-Huckel constant  $A^\phi$  were taken from Moller

(1988). Temperature functions for the acid-base binary parameters and mixing parameters in the H-Na-K-OH-Cl-H<sub>2</sub>O system were taken from Christov and Moller (2004a). These acid/base solution parameters fit the experimental  $K_w$  data in sodium and potassium chloride solutions with pH values  $\approx 1.5$  to 10 to  $I = 5\text{ m}$  with a very high accuracy from 0° to 250°C.

The many interrelated aluminum hydrolysis species present in the intermediate pH range make it difficult to decouple their parameterization. However for sufficiently low pH essentially all the aluminum in solution ( $Al_{tot}$ ) is in the  $Al^{3+}(aq)$  ion form. Similarly, for sufficiently high pH the  $Al_{tot}$  will be in the highest hydrolysis form, the aluminate ion,  $Al(OH)_4^-$  (see Eq's 10-13). Therefore the most complete data sets to model the interactions of MN aluminum species are those for  $Al^{3+}(aq)$  at low pH and those for  $Al(OH)_4^-$  at high pH. As a result, these ranges provide the most reliable parameterization of the model. To maximize the availability of data to describe the dramatic changes in solute composition occurring in this system, we staged the development of the model in different temperature and composition regions.

**5-2a. Parameterization of  $Al^{3+}$  Interactions in the Low pH H-Al-Na-K-Cl-H<sub>2</sub>O System (0° to 100°C):** We began the model by parameterizing the acid side at low temperature ( $T < 100^\circ C$ ), as described in Christov et al. (2007). For the pH region of this parameterization, it was assumed that the only aluminum species in solution was the  $Al^{3+}$  ion. The data available for constructing this model include electromotive force, osmotic and  $AlCl_3 \cdot 6H_2O(s)$  solubility studies in the  $AlCl_3$ -H<sub>2</sub>O,  $AlCl_3$ -NaCl-H<sub>2</sub>O,  $AlCl_3$ -HCl-H<sub>2</sub>O,  $AlCl_3$ -KCl-H<sub>2</sub>O and  $AlCl_3$ -KCl-NaCl-H<sub>2</sub>O systems ranging from 0° to 98°C. The parameters established as a function of temperature were:  $\beta^0_{Al,Cl}$ ,  $\beta^1_{Al,Cl}$ ,  $C^0_{Al,Cl}$ ,  $\theta_{Na,Al}$ ,  $\theta_{K,Al}$ ,  $\theta_{Al,H}$ ,  $\Psi_{H,Al,Cl}$ ,  $\Psi_{Na,Al,Cl}$  and  $\Psi_{K,Al,Cl}$ .

Figures 6ab compare the H- $Al^{3+}$ -K-Cl-H<sub>2</sub>O model and experimental solubility in the  $AlCl_3$ -KCl-H<sub>2</sub>O system at 0°, 25°, 40° and 80°C. The agreement obtained is very good. The largest difference between model and experiment occurs for the sylvite +  $AlCl_3 \cdot 6H_2O(s)$  invariant point in the  $AlCl_3$ -KCl-H<sub>2</sub>O system at 25°C for which the model predicts potassium concentrations that are about 18% lower than experiment (see Fig. 6b). However the model gives a solution composition for the invariant point in the ternary system at 25°C that is very close to the composition recommended by Patel and Seshardi (1966) (open triangle in Fig. 6b). The model predicts that the total chloride-ion concentration for halite + sylvite +  $AlCl_3 \cdot 6H_2O(s)$  saturated solutions smoothly increases with temperature from 0° to 120°C.

Figure 7 compares the calculated (solid lines) and experimental (symbols) sylvite and  $AlCl_3 \cdot 6H_2O(s)$  saturation fields in the HCl-KCl- $AlCl_3$ -H<sub>2</sub>O system at 0°C, 25°C, and 80°C. Data, taken from Linke (1958; 1965), are from Malquori (1927ab; 1928): ■, 0°C; □, 25°C; ○, 80°C and from Patel and Seshardi (1996): ●, 25°C. We could not find activity data (e.m.f., osmotic) or solubility data in the  $AlCl_3$ -NaCl-HCl-H<sub>2</sub>O system in the literature. Keeping the same constant value of the  $\theta(Al,Na)$  parameter as in Palmer and Wesolowski (1992), we evaluated a temperature function for the  $\psi(Na,Al,Cl)$  mixing parameter. Our parameterization yields good agreement with the gibbsite solubility measurements of Palmer and Wesolowski (1992) in low pH sodium chloride solutions (pH  $\approx 3$  to  $\approx 4.5$ ; 0.1- 5 mol.kg<sup>-1</sup> NaCl) from 30°C to 70°C. A preliminary temperature function for the gibbsite chemical potential for this low temperature range was established using these data.

Figure 8 compares model calculations (solid lines) of the  $Al^{3+}$  concentration in solutions in equilibrium with gibbsite as a function of pH (pH = -log [H<sup>+</sup>]) at 30°, 50° and

70°C and I (NaCl) = 5 m with the experimental Al<sup>3+</sup> vs. pH data (symbols) of Palmer and Wesolowski(1992). Palmer and Wesolowski (1993) determined the first hydrolysis constant of Al<sup>3+</sup> (Q<sub>H1</sub>; see Eq. 10) potentiometrically in sodium chloride solutions from 25° to 125°C. Using these results, Palmer and Wesolowski (1992) estimated that the effect of Al<sup>3+</sup> hydrolysis is not significant in their solubility experiments. We tested extrapolation of our low pH model to 100°C by showing good agreement of model predicted gibbsite dissociation constants (K<sub>so</sub>/Q<sub>so</sub>; see Eq. 17) with those reported by Wesolowski and Palmer (1994) at 100°C.

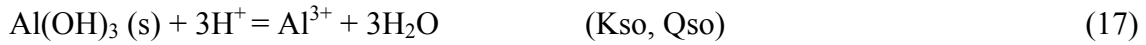


FIGURE 6a

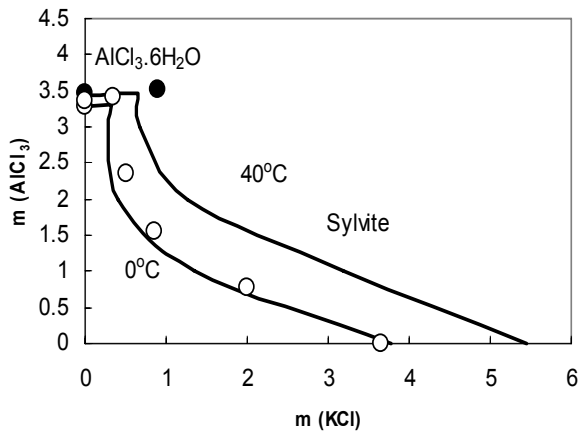


FIGURE 6b

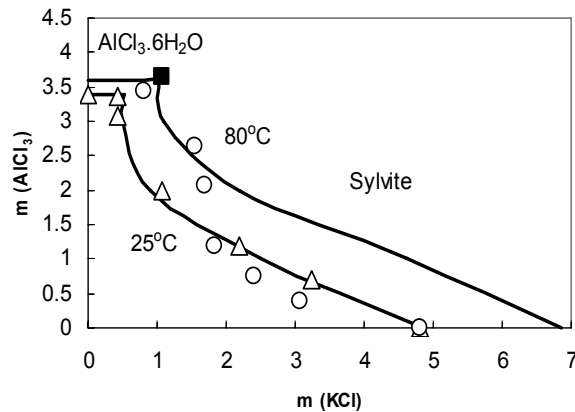


FIGURE 7

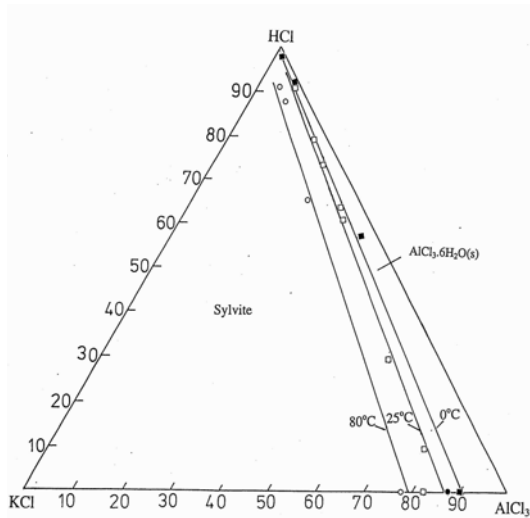
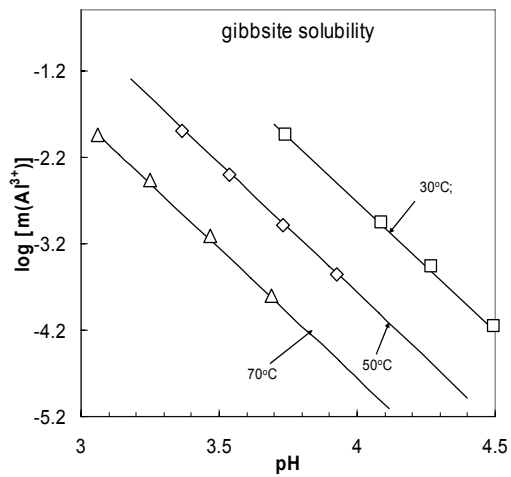


FIGURE 8



**5-2b. Parameterization of the Standard Chemical Potentials of the Aqueous  $\text{Al(OH)}^{2+}$ ,  $\text{Al(OH)}_2^+$ ,  $\text{Al(OH)}_3^0$  and  $\text{Al(OH)}_4^-$  Species (T: 0-300°C) and the Pitzer Interaction Parameters for  $\text{Al(OH)}_n$ ; n = 1-3 (T<100°C; 0-5 m NaCl) in the Intermediate pH Region:** In the intermediate pH range, the monoaluminum hydrolysis species ( $\text{Al(OH)}_n$ ; n = 1-4) are present in concentration ratios varying with pH according to the equilibria expressed by Eq.'s 10-13. The good accuracy of the parameterization in the low pH and low temperature region (T<100°C) discussed in section 5-2a (see also Christov et al 2007) allowed its use as a base for developing the parameterization for the low temperature, intermediate pH range.

We evaluated the standard chemical potentials of the hydrolysis species,  $\text{Al(OH)}^{2+}$ ,  $\text{Al(OH)}_2^+$ ,  $\text{Al(OH)}_3^0$ , and  $\text{Al(OH)}_4^-$  as well as the binary Pitzer parameters for  $\text{Cl}^-$  interactions with  $\text{Al(OH)}^{2+}$ ,  $\text{Al(OH)}_2^+$ , and  $\text{Al(OH)}_4^-$  and the Pitzer ternary parameters,  $\lambda_{\text{Al(OH)}_3, \text{Cl}}$  and  $\zeta_{\text{Al(OH)}_3, \text{NaCl}}$ , in the intermediate pH range at temperatures below 100°C using the Wesolowski and Palmer (1994) (smoothed) concentration products (see Eq's. 10-13) corresponding to the hydrolysis reactions (in 0-5 m NaCl solutions: n = 1 T< 125°C; n = 2-4, T<100°C). The standard chemical potential of  $\text{Al}^{3+}$  was set equal to zero. The Wesolowski and Palmer (1994) (smoothed) concentration products summarize the gibbsite solubility measurements of Wesolowski (1992) and Palmer and Wesolowski (1992) as well as the potentiometric measurements of Palmer and Wesolowski (1993). In the final model it is important to have a continuous variation in temperature of all the parameters for the entire temperature range of the model (T $\approx$  0 to  $\approx$  300°C). To facilitate this, we included the recommendations of Wesolowski and Palmer (1994) for the hydrolysis constants ( $K_{\text{Hn}}$ ; see Eq's 10-13) for n = 2-4 for T >100°C and for n = 1 for T >125°C in the data base. Testing showed that many parameters could be set equal to zero in this parameterization without significantly affecting the accuracy of the fit.

Extrapolations with temperature (see Eq. 15) of these low temperature Pitzer parameters for the low and intermediate pH range were used to define low and intermediate pH behavior in the high temperature region (T>100°C to  $\approx$  300°C) where there are very few reliable data. However, some modifications of these extrapolations were necessary in the final model to increase the agreement with the high temperature, high pH data (see section 5-2c). For example, this evaluation of the (n = 4)  $\text{Al(OH)}_4^-$  Pitzer interaction parameters was modified in the final model (see section 5-2c). This will be discussed in more detail in the publication of this work (in preparation).

The above solution model for the low temperature intermediate region was validated using the gibbsite solubility measurements of Wesolowski and Palmer (1994) that cover the entire pH region (pH = 3-9) at 50°C. Using a Gibbs free energy of reaction for gibbsite obtained from data in the high pH region (discussed in the next section, 5-2c), the solubility of this mineral in the entire pH region at 50°C can be predicted using the solution parameterization described in this section (see Fig. 9).

**5-2c. Parameterization of the  $\text{Al(OH)}_4^-$  Aqueous Species Interactions and the Gibbs Free Energies of Reaction for the Minerals, Gibbsite and Boehmite, in the High pH Region (0- 300°C):** The parameters for the important base side solution species  $\text{Al(OH)}_4^-$  ( $\beta^0$ ,  $\beta^1$ ,  $\beta^2$  for  $\text{Al(OH)}_4^-$ -  $\text{Na}^+$  interactions,  $\theta_{\text{OH}, \text{Al(OH)}_4}$  and  $\psi_{\text{Na}, \text{OH}, \text{Al(OH)}_4}$ ) and the Gibbs free energies of reaction for the minerals, gibbsite and boehmite, were evaluated in the high pH region using solubility measurements and osmotic data. Both high and low



temperature data were fit simultaneously. For  $T < 100^\circ\text{C}$ , we used the gibbsite solubility data of Wesolowski et al (1992;  $6.4^\circ$  to  $80^\circ\text{C}$ ) in NaOH (.0095 to 2.8  $m$ ) and NaCl (to 5.0  $m$ ). The  $25^\circ\text{C}$  osmotic data of Park and Englezos (1999) and the  $40.05^\circ\text{C}$  osmotic data of Zhou et al (2003) were also included in the data base. For temperatures above  $100^\circ\text{C}$  gibbsite becomes unstable. However, for this high temperature range there is a considerable body of well determined boehmite solubility data to high pH that can be used for parameterization and validation. We used the solubility measurements of Castet et al. (1993) from  $170^\circ$  to  $250^\circ\text{C}$  ( $\text{pH} > 8.0$ ), which had very low concentrations (.01  $m$  NaCl + NaOH), as well as the solubility measurements of Diakonov et al (1996) from  $125^\circ$  to  $250^\circ\text{C}$  at 1  $m$  NaCl. These data sets were selected because they provide the initial solution compositions and total aluminum concentrations, and we were interested in the possibility of ion association between the  $\text{Na}^+$  and the  $\text{Al}(\text{OH})_4^-$  ions..

In fitting the data ( $\approx 0^\circ$  -  $300^\circ\text{C}$ ), we found that the  $\beta^2$  parameter became large and negative at high temperature. This is consistent with the use of an associated  $\text{NaAl}(\text{OH})_4(\text{aq})$  ion species in the analysis of Diakonov et al (1996). However, for the level of association found we have shown that specific interaction model can provide better accuracy (Harvie et al. 1984). This will be discussed in the publication in preparation.

Standard chemical potential values for the solids, gibbsite,  $\mu_{\text{Al}(\text{OH})_3(\text{cr})}^\circ(T)$ , and boehmite,  $\mu_{\text{AlOOH}(\text{cr})}^\circ(T)$ , can be calculated from the free energies of reaction of these species using the standard chemical potential of  $\text{Al}(\text{OH})_4^-$ ,  $\mu_{\text{Al}(\text{OH})_4}^\circ(T)$ , determined in the fit to the  $\text{Q}_{\text{H}4}$  data ( $T < 100^\circ\text{C}$ ) and the  $K_{\text{H}4}$  recommendations of Wesolowski et al (1994) ( $T > 100^\circ\text{C}$ ) (see section 5-2b). Using these solid phase potentials and the solution model, the good agreement of model predictions with solubility data in the high pH region is illustrated for gibbsite in Fig. 9 below.

FIGURE 9

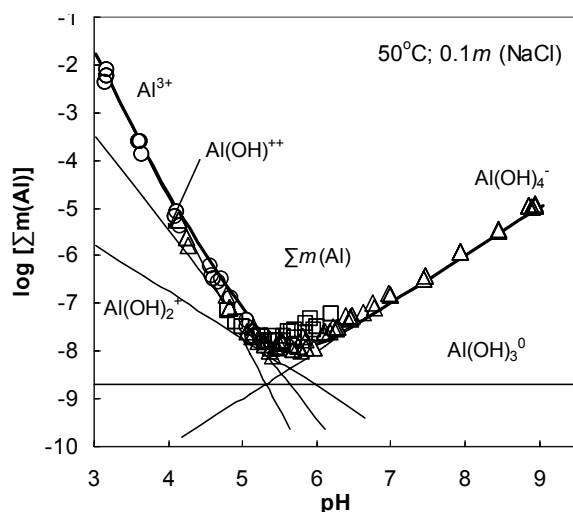


FIGURE 10

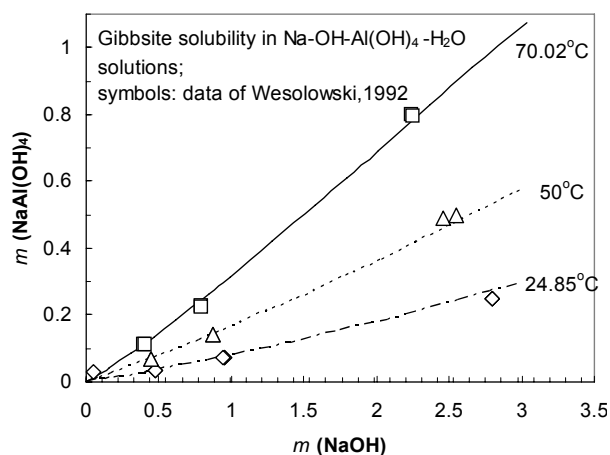


Fig. 9. Model predicted molal concentrations ( $m = \text{mol}\cdot\text{kg}^{-1}$ ) of the monoaluminum hydrolysis  $\text{Al}_x(\text{OH})_y^{3x-y}$  species (light straight lines) in solutions in equilibrium with gibbsite as a function of pH ( $\text{pH} = -\log[\text{H}^+]$ ) at  $50^\circ\text{C}$  and  $I(\text{NaCl}) = 0.1 m$ . The symbols show the experimental total molality Al (total) vs. pH data of Wesolowski and Palmer (1994) measured in different buffers (o, acetate; Δ, tris; □, bistris). The solid curved line is the model predicted total concentration of all aqueous aluminum species.

Fig. 10. The  $\text{NaAl(OH)}_4^-$  concentration ( $m = \text{mol.kg}^{-1}$ ) in solutions in equilibrium with gibbsite as a function of NaOH concentration at 24.85°, 50° and 70.02°C. The symbols show the experimental  $m$  ( $\text{NaAl(OH)}_4^-$ ) vs.  $m$  (NaOH) data of Wesolowski (1992). The lines represent the predictions of the gibbsite solid-liquid equilibrium model presented here..

**5-2d. Final pH Dependent Model to High Temperature and to High NaCl Concentration:** In the previous sections the evaluation of the solution model (Pitzer parameters and standard chemical potentials of aqueous species) for temperatures from  $\approx 0$  to  $100^\circ\text{C}$  with a pH range from  $\approx 1.5$  to  $\approx 10$  and for temperatures from  $0$  to  $\approx 300^\circ\text{C}$  for high pH ( $> 8.0$ ), and the chemical potentials of gibbsite from  $0$  to  $100^\circ\text{C}$  and boehmite from  $100^\circ\text{C}$  to  $\approx 300^\circ\text{C}$  have been discussed. The development of the solution model for the high temperature ( $T > 100^\circ\text{C}$ ) and low to intermediate pH range remains to be considered. For this high temperature range, even at low pH there are many coexisting aluminum hydrolysis species each requiring several interaction parameters. In addition there are relatively few consistent well defined data.

To develop a predictive model for this region we adopted the following strategy. We extrapolated the low temperature parameterization of the low and intermediate pH regions described in sections 5-2a and 5-2b to high temperatures and achieved excellent agreement (see Fig's 11 and 12) with the total aluminum vs. pH measurements at high temperature and low ionic strength of Benezeth et al. (2001) ( $0.03\ m\ \text{NaCl}$ ;  $101.5^\circ\text{-}290.2^\circ\text{C}$ ) and Caset et al. (1993) ( $.01\ \text{NaCl}$ ;  $150^\circ\text{C}$  to  $350^\circ\text{C}$ ). This agreement, which can't be improved with the current data situation, supports the quality of the extrapolated standard chemical potentials in the model. Therefore, we retained these extrapolations in the final model.

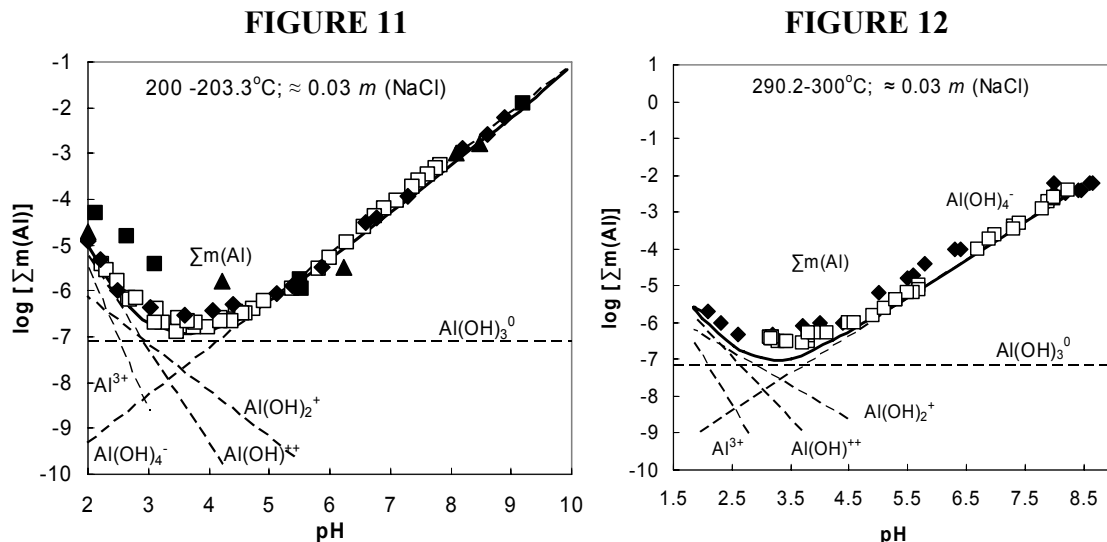


Fig. 11: Left  $T \approx 200^\circ\text{C}$  and Fig. 12: Right  $T \approx 300^\circ\text{C}$ . ( $\text{NaCl} = 0.03\ m$ ). Model prediction of  $\text{Al(OH)}_y^{3x-y}$  species (dashed straight lines) concentrations in solutions in equilibrium with boehmite as a function of pH ( $\text{pH} = -\log [\text{H}^+]$ ). The solid curve model predictions of total aluminum. Symbols  $\blacksquare$  data of Kuyonko et al. (1983),  $\blacktriangle$  data of Bourcier et al. (1993),  $\blacklozenge$  data of Castet et al. (1993).

However, for high temperatures (from 152.4° to 254°C) and high molality (0.1 – 5 *m* NaCl), the extrapolated interaction parameters yield slightly higher boehmite solubility than measured by Palmer et al. (2001) in the low pH range. To improve the agreement of the model in this region we slightly modified the high temperature ( $T > 125^\circ\text{C}$ ) extrapolation of the binary parameters  $\beta^1_{\text{Al,Cl}}$ ,  $\beta^1_{\text{Al(OH),Cl}}$  and  $\beta^1_{\text{Al(OH)}_2,\text{Cl}}$  and the  $\psi_{\text{Al,Na,Cl}}$  ternary mixing interaction parameter. The temperature variation was constrained to retain the parameterization at lower temperatures ( $T < 100^\circ\text{C}$ ). The new temperature dependant parameters considerably improve the fit of the Palmer et al. (2001) data at low pH. In the intermediate pH region, the predicted  $\text{Al}_{\text{tot}}$  values from the extrapolated model were also slightly higher than the data. To improve the behavior of the model in this region the high temperature variation of the ternary neutral species parameters  $\lambda_{\text{Al(OH)}_3,\text{Cl}}$  and  $\xi_{\text{Al(OH)}_3,\text{NaCl}}$  were adjusted to fit the high temperature and high ionic strength boehmite solubility,  $Q_{\text{S3}}$ , data of Palmer et al (2001) again constraining the temperature to preserve as much as possible the low temperature variation of the original data fit. Examples of predictions of the final model at high temperature for concentrated solutions with pH values from  $\approx 2.0$  to  $\approx 9.5$  are given in Fig's. 13 and 14 and are very satisfactory. The closed circle in Fig. 13 represents the high concentration data of Diakonov et al.(1996) (see section 5-2c).

FIGURE 13

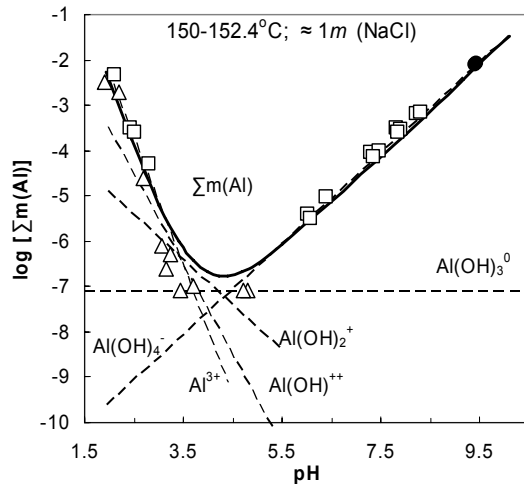


FIGURE 14

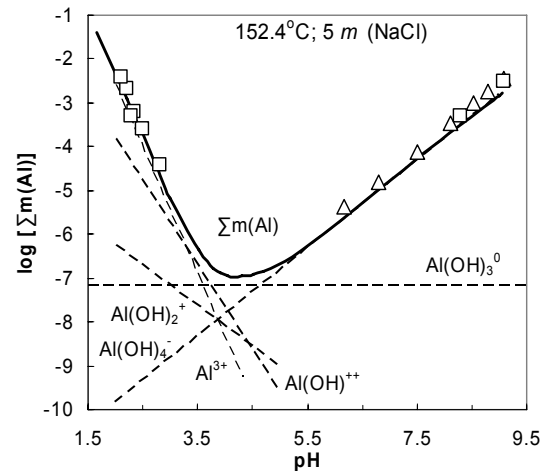


Fig. 13: Left,  $I \approx 1m$ , Fig. 14: Right,  $I \approx 5m$ , Model predictions of  $\text{Al(OH)}_y^{3x-y}$  species concentrations (dashed straight lines) in solutions in equilibrium with boehmite vs. pH ( $\text{pH} = -\log [\text{H}^+]$ ) at  $T \approx 150.0^\circ\text{C}$ . Solid lines are the model prediction of the total aluminium concentration. Open symbols.  $\square, \Delta$ , represent data of Palmer et al. (2001) (for various runs).  $\bullet$  data of Diakonov et al. (1996) at  $150^\circ$ .

**5-2e. Potassium Interactions in the  $\text{H}^+ - \text{K}^+ - \text{Na}^+ - \text{Cl}^- - \text{OH}^- - \text{Al}^{3+} - \text{Al(OH)}^{2+} - \text{Al(OH)}_2^+ - \text{Al(OH)}_3 - \text{Al(OH)}_4^- - \text{H}_2\text{O(l)}$  System (0 to  $\approx 100^\circ\text{C}$ ):** With the variable temperature ( $\approx 0^\circ - 300^\circ\text{C}$ ) model of the  $\text{H} - \text{Na} - \text{Al}^{3+} - \text{Al(OH)}^{2+} - \text{Al(OH)}_2^+ - \text{Al(OH)}_3^0 - \text{Al(OH)}_4^- - \text{Cl} - \text{OH} - \text{H}_2\text{O}$  system completed, we began work on incorporating the aluminum-potassium interactions in this model so that we can predict the dissolution/solution behavior of the important

potassium aluminosilicate hydrothermal minerals. The Na-Cl, Na-OH, K-Cl and K-OH binary interaction parameters and the  $\theta_{\text{OH,Cl}}$ ,  $\theta_{\text{Na,K}}$ ,  $\theta_{\text{K,H}}$ ,  $\psi_{\text{Na,K,Cl}}$ ,  $\psi_{\text{Na,OH,Cl}}$ ,  $\psi_{\text{K,OH,Cl}}$  and  $\psi_{\text{K,Na,OH}}$  mixing parameters have been determined previously (see Christov and Moller, 2004a).

There are much fewer experimental data available to parameterize the influence of  $\text{K}^+$  ions on the  $\text{Al}^{3+}$  hydrolysis reactions than were found for the  $\text{Na}^+$  interactions. However, the Pitzer formulism supports the transfer of parameter values between systems. Therefore all the evaluations for the  $\text{Cl}^-$  binary interaction parameters with  $\text{Al}^{3+}$  and the aluminium hydrolysis species, the potassium-free mixing parameters (e.g.,  $\theta_{\text{OH,Al(OH)}_4}$ ) and the temperature functions for the standard chemical potentials of  $\text{Al}^{3+}$  (equal to 0),  $\text{Al(OH)}^{2+}$ ,  $\text{Al(OH)}_2^+$ ,  $\text{Al(OH)}_3^0$ ,  $\text{Al(OH)}_4^-$ , and solid gibbsite determined in the sodium system can be transferred to the potassium model. The parameters  $\theta_{\text{K,Al}}$  and  $\psi_{\text{K,Al,Cl}}$  were evaluated using low pH data where the  $\text{Al}^{3+}$  species dominates in the KCl system (see section 5-2b and Christov, Dickson and Moller (2007). Agreement with these data is shown in Figs. 7ab and 8.

The only data we found involving potassium interactions with aluminum hydrolysis species are the gibbsite solubility measurements of Wesolowski (1992) measured in high pH potassium-aluminum solutions, K-OH-Al(OH)<sub>4</sub>-H<sub>2</sub>O and Na-K-OH-Al(OH)<sub>4</sub>-H<sub>2</sub>O, from  $\approx 25^\circ$  to  $70^\circ\text{C}$ . These data range in potassium hydroxide molality from 0.008 to 2.268 *m* and in potassium aluminate molality from 0.0006 to 0.38 *m*. On the basis of his results, Wesolowski (1992) concluded that gibbsite solubility as function of temperature and ionic strength in KOH and NaCl + KCl solutions is nearly identical to the equivalent values in NaOH and NaCl solutions. Using the Wesolowski data, we evaluated the K-Al(OH)<sub>4</sub> binary interaction parameters and the mixing parameters,  $\psi_{\text{K,OH,Al(OH)}_4}$ . Model predictions are in good agreement with the gibbsite solubility data both the sodium and potassium systems (see Fig's 15ab). Other aluminum-potassium interaction parameters could be set to zero without affecting the agreement with the data.

FIGURE 15a

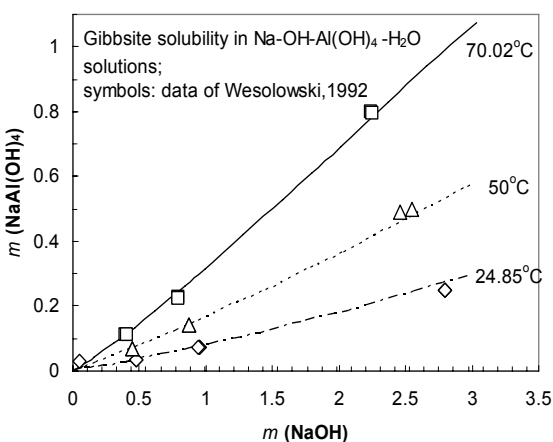
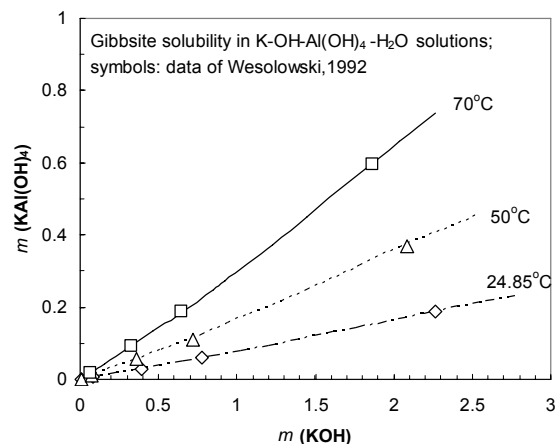


FIGURE 15b



**5-2f. Summary: A Predictive pH Dependent Model of Solution-Solid Equilibria in the  $\text{H}^+$ - $\text{K}^+$ - $\text{Na}^+$ - $\text{Cl}^-$ - $\text{OH}^-$ - $\text{Al}^{3+}$ - $\text{Al(OH)}^{2+}$ - $\text{Al(OH)}_2^+$ - $\text{Al(OH)}_3$ - $\text{Al(OH)}_4^-$ - $\text{H}_2\text{O(l)}$  System to High Salt Concentration and Temperature:** Because of its importance to many

problems in geothermal, geological, and environmental chemistry, this system has been the subject of many investigations. The model presented here provides predictions with accuracy close to that of the data in the  $\approx 1.5$  to  $\approx 10$  pH range, to high concentrations (5 m) of NaCl and KCl (salts commonly found in natural waters) to high temperature (NaCl:  $\approx 0^\circ$  to  $\approx 300^\circ\text{C}$ ; KCl:  $T \leq 100^\circ\text{C}$ ). The ionic and neutral solute species interactions in the model are described by the Pitzer specific interaction mixing model. A significant result of this study is the illustration of the accuracy of this phenomenology in describing the complex chemistry of this system for such large ranges of the intensive variables: pH, salt concentration and temperature. We believe that this is a major advancement in the ability to characterize the important aluminium aqueous chemistry that plays a central role in many rock/fluid interactions. The results of the extensive validation of the model against the available data are documented in the prior sections.

Interesting insight into the chemical behavior of this important system can be obtained from model predictions. Examples are shown in Fig's 16ab, which illustrate the distribution of Al aqueous species as a function of pH for the low total aluminium solutions typical of natural waters. At low temperature (Fig. 16a), although the neutral species,  $\text{Al}(\text{OH})_3^0$ , contributes to the total aluminum concentration substantially in the intermediate pH, it does not dominate. On the other hand, at higher temperature (Fig. 16b), the neutral species clearly dominates. The solid vertical lines represent the neutrality of pure water.

FIGURE 16a

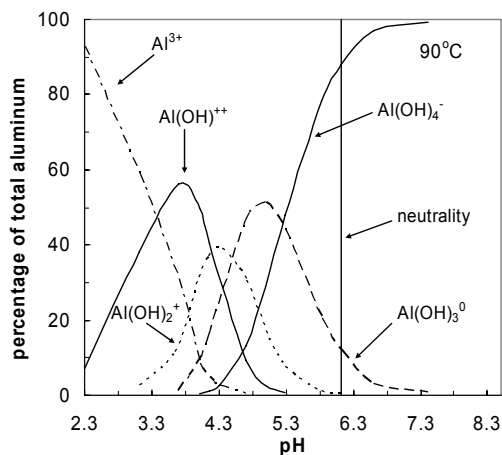
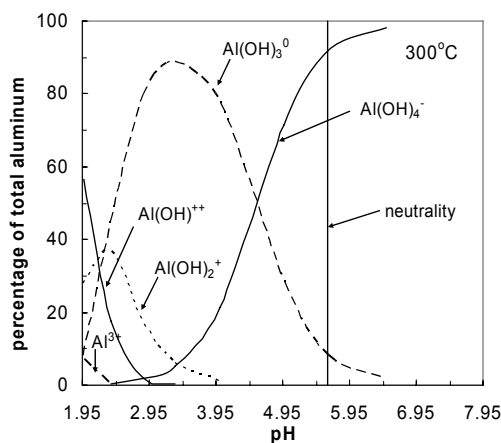


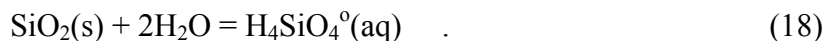
FIGURE 16b



### 5-3. MODEL OF SILICA AQUEOUS CHEMISTRY AND SILICA SOLID PHASES

With funding from our previous DOE geothermal grant, we updated our earlier TEQUIL silica model which described interactions of the neutral  $\text{H}_4\text{SiO}_4^0(\text{aq})$  species in brines to high temperature. We added silica acid-base solution reactions and quartz ( $\text{SiO}_2(\text{s})$ ) to the model as well as several new temperature functions for  $\text{H}_4\text{SiO}_4(\text{aq})$  interactions with Na, K, Ca, Cl and  $\text{SO}_4$ . At the low silica concentrations typically found in geothermal waters, silica exists as the monomeric neutral  $\text{H}_4\text{SiO}_4^0$  species and its acid dissociation products over

a wide temperature range (Busey and Mesmer (1977); Gout et al. (2000, Raman spectroscopy data). At 20°C, for example, roughly 4% of silica in solution still exists as  $\text{H}_4\text{SiO}_4^\circ(\text{aq})$  even at  $\text{pH} = 11$ . The solubility of the quartz and amorphous silica solid phases is controlled by the activity of  $\text{H}_4\text{SiO}_4^\circ(\text{aq})$  and a model of silica mineral solubility may be formulated using the mass balance activity expression (Eq. 18),



Added salt dramatically changes the  $\text{H}_4\text{SiO}_4$  weak acid behavior. For high salinity brines ( $\text{NaCl} = 5 \text{ m}$ ),  $\text{pK}_1$  values decrease dramatically with temperature. At high temperature there is a substantial amount of acid dissociation even under moderate pH conditions. When the  $\text{H}_4\text{SiO}_4^\circ(\text{aq})$  species dissociates, the solubility equilibrium moves to the right in Eq. 18. Therefore, for high salinity brines it was necessary to develop an acid/base silica model.

To evaluate standard chemical potential temperature functions for amorphous silica and cristobalite, we used the solubility  $\ln K$  values proposed by Gunnarsson and Arnorsson (2000). Their  $\ln K$  constants are valid from 0° to 250°C. We use the  $\ln K$  constants of Arnorsson et al. (1982a) to evaluate standard chemical potential functions for chalcedony (25° to 180°C). Their temperature  $\ln K$  function corresponds well with the chalcedony solubility data of Fournier (1973). In Fig's.17-19, we compare model prediction (solid lines) and the data (symbols) for the pure water solubility of amorphous silica, cristobalite and chalcedony. In all three figures the open squares represent mineral solubilities calculated from the  $\ln K$  solubility constants of Gunnarsson and Arnorsson (2000) for amorphous silica, and cristobalite and of Arnorsson et al. (1982a) for chalcedony. Also shown in Fig. 24 are the pure water amorphous silica solubility data of Gunnarsson and Arnorsson (2000) (open diamonds) from 8° to 250°C and the amorphous silica ( $\text{SiO}_2 \cdot 2\text{H}_2\text{O}(\text{cr})$ ) solubility data of Marshall (1980) (open triangles). The cristobalite and chalcedony models give an excellent agreement with the Gunnarsson and Arnorsson (2000) and Arnorsson et al. (1982a) solubility data. The amorphous silica ( $\text{SiO}_2(\text{cr})$ ) model is also in excellent agreement with the all three sets of data from 0° to 150°C. At higher temperature the model predicts a little higher (6% or less) solubility than the data of Marshall (1980) (max diff. of 0.0011 *m* at 200°C). The predicted amorphous silica solubility at temperature over 150°C is also higher (13% or less) than the raw data of Gunnarsson and Arnorsson (2000) (max diff. of 0.0024 *m* at 200°C).

FIGURE 17

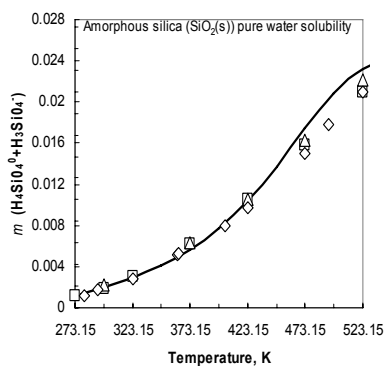


FIGURE 18

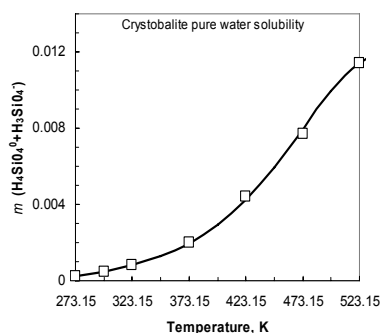
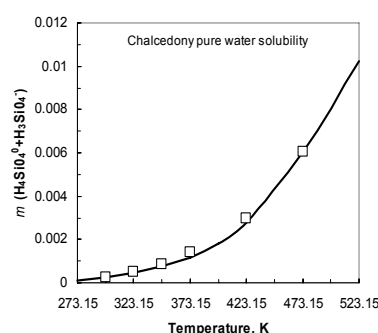


FIGURE 19



## 5-4 ADDITION OF ALUMINOSILICATE SOLID PHASES TO MODEL

Aluminosilicates are the major rock forming minerals in the earth's crust and are consequently very important hydrothermal minerals controlling geothermal resource chemistry. Quartz is also a common component of geothermal reservoir formations. In order to interpret the effects of injection or hydrothermal fluid interactions on the permeability of formations containing these minerals, we need to be able to estimate the activities of all the species in their dissolution reactions.

With the development of a model of aqueous aluminum chemistry in the H-Na-K-OH-Cl-Al<sup>3+</sup>-Al(OH)<sup>2+</sup>-Al(OH)<sub>2</sub><sup>+</sup>-Al(OH)<sub>3</sub><sup>0</sup>-Al(OH)<sub>4</sub><sup>-</sup>-H<sub>2</sub>O system (NaCl: 0° - 300°C; KCl: 0°-100°C) under this grant (see above), our comprehensive suite of TEQUIL solution models includes components necessary to describe the saturation status of hydrothermal fluids in contact with many important aluminosilicate minerals (see those compiled in the report of Browne (Browne, 1978) for the temperature, pressure, and concentration conditions encountered in many geothermal applications. Given the standard free energies of reaction of the solid phases as a function of temperature, the saturation status of hydrothermal brines within the H<sup>+</sup>, Na<sup>+</sup>, K<sup>+</sup>, Al<sup>3+</sup>, Cl<sup>-</sup>, Si(OH)<sub>4</sub>, SiO(OH)<sub>3</sub><sup>-</sup>, OH<sup>-</sup>, Al(OH)<sup>2+</sup>, Al(OH)<sub>2</sub><sup>+</sup>, Al(OH)<sub>3</sub><sup>0</sup>, Al(OH)<sub>4</sub><sup>-</sup>, H<sub>2</sub>O system can be calculated with respect to minerals in this system (see Table 3) Data sources are also given in Table 3.

Unfortunately, the availability of data for directly calculating the Gibbs free energy of aluminosilicate minerals is poor. Therefore we must rely on thermodynamic data bases available in the literature to calculate the free energy of reaction of most of these minerals. To calculate the solubility of aluminosilicate minerals, our silica and aluminum solution models must be compatible with each other and with the methods used to calculate the thermodynamic data bases. To check our approach and these compatibilities, we started with the few minerals that have both free energy data and solubility data.

Kaolinite (Al<sub>2</sub>Si<sub>2</sub>O<sub>5</sub>(OH)<sub>4</sub>), a common hydrothermal aluminosilicate mineral, has some data available to check the modeling approach and results. We used the kaolinite dissociation constants established in alkaline solutions (K<sub>s4</sub>; see Eq. 19 below) of Devidal et al. (1996) as well as the K<sub>s4</sub> values determined by other authors (200°C: Mukhamed-Galeev and Zotov (1992) and Huang (1993); 250°: Hemley et al. (1980)) to evaluate a temperature function for the kaolinite free energy of reaction from 0°C to 250°C.

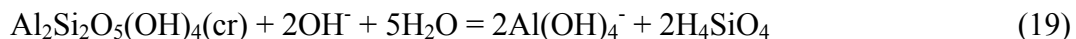


Figure 20 shows that our model is in excellent agreement to high temperature with the Devidal et al. K<sub>s4</sub> data, the 200°C of Huang (closed circle) and the 250°C data of Hemley et al. (open diamond). It is in good agreement with the 25°C data of Barany and Kelley (1961) (open triangle). However, the kaolinite model predicts lower K<sub>s4</sub> values than those given by Huang and Keller (1973) (25°: crosses), Helgeson et al. (1978) (25°C: close diamond) and Nagy et al. (1981) (80°C: open circle). The model value lies between the two 200°C points of Mukhamed-Galeev and Zotov (1992) (200°C, stars).

**TABLE 3**

<b>MINERAL</b>	<b>DATA SOURCE</b>
<b>Al (III) Minerals</b>	
Aluminum chloride hexahydrate: $\text{AlCl}_3 \cdot 6\text{H}_2\text{O}(\text{s})$	Solubility data in $\text{AlCl}_3\text{-H}_2\text{O}$ system (Linke, 1965)
Gibbsite: $\text{Al}(\text{OH})_3(\text{s})$	Raw solubility data (Wesolowski, 1992; Palmer and Wesolowski, 1992; Wesolowski and Palmer, 1994)
Boehmite: $\text{AlOOH}(\text{s})$	Raw solubility data (Castet et al., 1993; Diakonov et al., 1996; Benezeth et al., 2001; Palmer et al., 2001)
<b>Si (IV) Minerals</b>	
Quartz: $\text{SiO}_2(\text{s})$	Pure water solubility data; Solubility data in NaCl solutions (Hemley et al., 1980); Log K values of Gunarsson and Arnorsson (2000)
Chalcedony: $\text{SiO}_2(\text{s})$	Log K values of Arnorsson et al. (1982)
Cristobalite: $\text{SiO}_2(\text{s})$	Log K values of Gunarsson and Arnorsson (2000)
Amorphous silica: $\text{SiO}_2(\text{s})$	Log K values of Gunarsson and Arnorsson (2000)
Amorphous silica: $\text{SiO}_2 \cdot 2\text{H}_2\text{O}(\text{s})$	Solubility data of Marshall and co-workers (1980-1982)
<b>Al(III)-Si (IV) Minerals</b>	
Kaolinite: $\text{Al}_2\text{Si}_2\text{O}_5(\text{OH})_4(\text{s})$	Solubility data and Log K values of Devidal et al. (1996)
Dickite: $\text{Al}_2\text{Si}_2\text{O}_5(\text{OH})_4(\text{s})$	Solubility data of Zotov et al. (1998); $\Delta_r G_m^\circ$ value of Fialips et al. (2003)
<b>Na(I)-Al(III)-Si (IV) Minerals</b>	
Low albite: $\text{NaAlSi}_3\text{O}_8(\text{s})$	Log K values of Arnorsson and Stefansson (1999)
High albite: $\text{NaAlSi}_3\text{O}_8(\text{s})$	Log K values of Arnorsson and Stefansson (1999)
<b>K(I)-Al(III)-Si (IV) Minerals</b>	
Microcline: $\text{KAlSi}_3\text{O}_8(\text{s})$	Log K values of Arnorsson and Stefansson (1999)
Sanidine: $\text{KAlSi}_3\text{O}_8(\text{s})$	Log K values of Arnorsson and Stefansson (1999)
<b>Sodium and Potassium Zeolites (to be included)</b>	
Analcime 1 (Si/Al = 2.0): $\text{NaAlSi}_2\text{O}_6 \cdot \text{H}_2\text{O}(\text{s})$	Log K values of Wilkin and Barnes (1998)
Analcime 2 (Si/Al = 2.5): $\text{Na}_{0.85}\text{Al}_{0.85}\text{Si}_{2.15}\text{O}_6 \cdot \text{H}_2\text{O}(\text{s})$	Log K values of Wilkin and Barnes (1998)
Na-clinoptilolite (Si/Al = 4.5): $\text{Na}_{1.1}\text{Al}_{1.1}\text{Si}_{4.9}\text{O}_{12} \cdot 3.5\text{H}_2\text{O}(\text{s})$	Log K values of Wilkin and Barnes (1998)
K-clinoptilolite (Si/Al = 4.5): $\text{K}_{1.1}\text{Al}_{1.1}\text{Si}_{4.9}\text{O}_{12} \cdot 2.7\text{H}_2\text{O}(\text{s})$	Log K values of Wilkin and Barnes (1998)



FIGURE 20

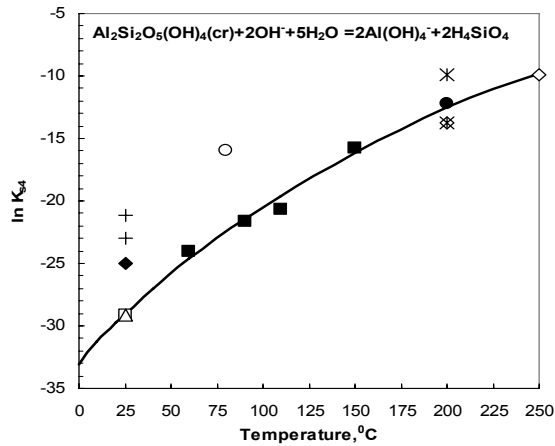


FIGURE 21

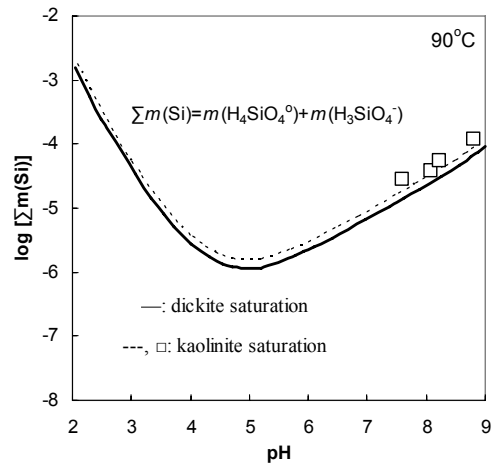


FIGURE 22

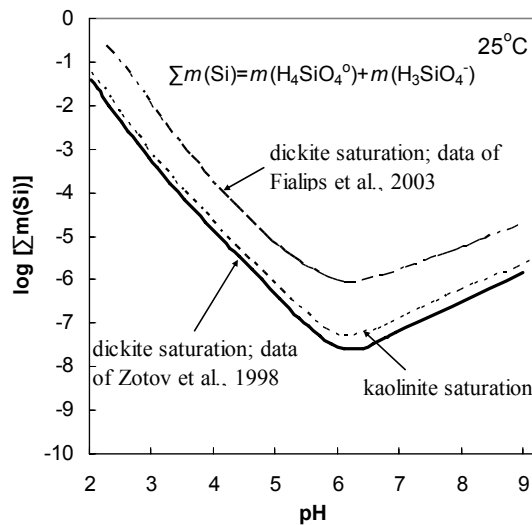
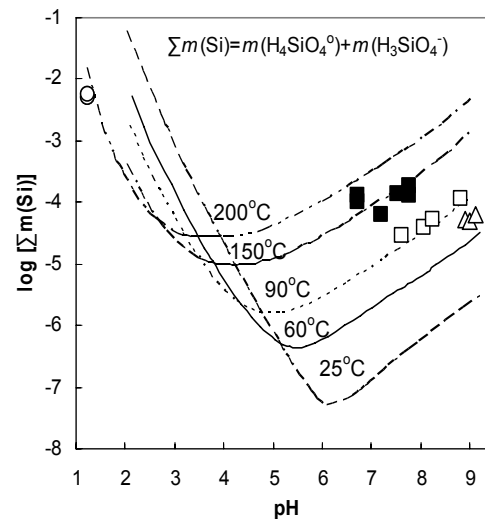


FIGURE 23



Devidal et al. (1996) also measured the solubility of kaolinite in alkaline solutions (60°C-160°C). Our model is in good agreement with these solubility data using this function for the kaolinite free energy of reaction. Fig. 21 shows the good agreement of the model (dashed line) with the Devidal et al. (1996) high pH (pH ≈ 7-9) kaolinite solubility data (open squares) at 90°C. Also shown in Fig. 21 is the model prediction of dickite solubility, a  $\text{Al}_2\text{Si}_2\text{O}_5(\text{OH})_4$  polymorph of kaolinite, (see solid line) established using the Gibbs free energy of reaction data of Zotov et al. (1998). There is some controversy in the literature about the relative stability of kaolinite and dickite, and the few thermodynamic data available for this salt vary widely. Figure 22 shows the calculated total silicate concentration ( $\Sigma m(\text{Si}) = m(\text{H}_4\text{SiO}_4^0) + m(\text{H}_3\text{SiO}_4^-)$ ) in equilibrium with dickite at 25°C using standard free energy

data ( $\Delta_f G^\circ_m(298\text{ K}, \text{ dickite})$ ) from Zotov et al. (1998) (solid line) and from Fialips et al. (2003) (dashed line). The dotted line is the model prediction of kaolinite solubility. This figure illustrates the variability of solubility predictions resulting from differences in reported free energies.

Figure 23 shows the calculated total silica concentration ( $\sum m(\text{Si}) = m(\text{H}_4\text{SiO}_4^0) + m(\text{H}_3\text{SiO}_4^+)$ ) of infinitely dilute solutions in equilibrium with kaolinite (lines) as a function of pH ( $\text{pH} = -\log a_{\text{H}^+}$ ) and temperature ( $25^\circ\text{C} - 200^\circ\text{C}$ ). The symbols  $\Delta$ ,  $\square$ , and  $\blacksquare$  represent the high pH experimental kaolinite solubility data of Devidal et al. (1996) at  $60^\circ\text{C}$ ,  $90^\circ\text{C}$  and  $150^\circ\text{C}$ , respectively. The  $\circ$  symbols show the low pH kaolinite solubility data of Zotov et al. (1998) at  $200^\circ\text{C}$ . Note the sharp difference in the solubility temperature dependence in the low pH region (solubility decreases with temperature) vs. the high pH region (increases with temperature). The agreement between model prediction and the raw experimental data is excellent. Note that the temperature function of the kaolinite free energy was evaluated only on the basis of the infinite dilution equilibrium constant ( $K_{s4}$ ) of the kaolinite dissociation reaction in alkaline solutions. Given the scarcity of the available solubility data, this result is important because it suggests that successful extrapolation of the model calculated solubilities over large pH ranges is possible even in systems with complicated temperature and pH dependent behavior.

Sodium and potassium feldspars and pure silica minerals (see section 5-3) are some of the most common hydrothermal formation minerals. Arnorsson and Stefansson (1999) compiled and assessed calorimetric and other thermodynamic data for the sodium and potassium feldspars. Using this thermodynamic database the authors derived temperature equations that describe the solubility constants ( $K$ ) (Eq. 20) for fully ordered sodium (low-albite and high-albite) and potassium (microcline and sanidine) feldspars in the temperature range from  $0^\circ$  to  $350^\circ\text{C}$ . We used the recommended  $K$  data of Arnorsson and Stefansson (1999) from  $0^\circ$  to  $300^\circ\text{C}$  to derive temperature functions for the standard chemical potentials for the fully ordered sodium feldspars, low-albite and high-albite, and for the potassium feldspars, microcline and sanidine.



To illustrate the capabilities of our thermodynamic model to describe brine/solid interactions in geothermal systems, we calculated the solubility diagrams for subsystems in our 12 component system model. In Fig. 24 the predicted solubility of sanidine in solutions containing high-albite at  $100^\circ\text{C}$  is illustrated. The total composition of any system on this diagram can be written in terms of the compositions of the minerals. The actual composition of the solution phase will be distributed according to the complex speciation scheme included in the model. In geothermal applications knowledge of mineral phase stability in highly concentrated salt solutions is often required. To illustrate feldspar mineral coexistence with solutions with varying dissolved salt concentration, we show in Fig. 25 the dissolved aluminum concentration at the invariant points of the low (low-albite/microcline) and high (high-albite/sanidine) plagioclases at  $100^\circ\text{C}$  in a solution initially containing only NaCl (initial NaCl concentrations in the solution are given on the axis). The flow of a NaCl rich brine through a formation of coexisting high-albite and sanidine will convert the sanidine to albite, substantially changing the Na/K concentration ratios in the solution phase even though

the amount of mineral dissolved is small. For example, in Fig. 25 when a 1 *m* NaCl aqueous solution was equilibrated with excess amounts of the sanidine and high-albite solid phases at 100°C 0.015 moles of K were transferred to the solution. However, the total aluminum in solution remained at  $\approx 1.7 \times 10^{-5} m$ . Since the volumes of minerals are different, this replacement process could significantly affect the pore volumes in the reservoir.

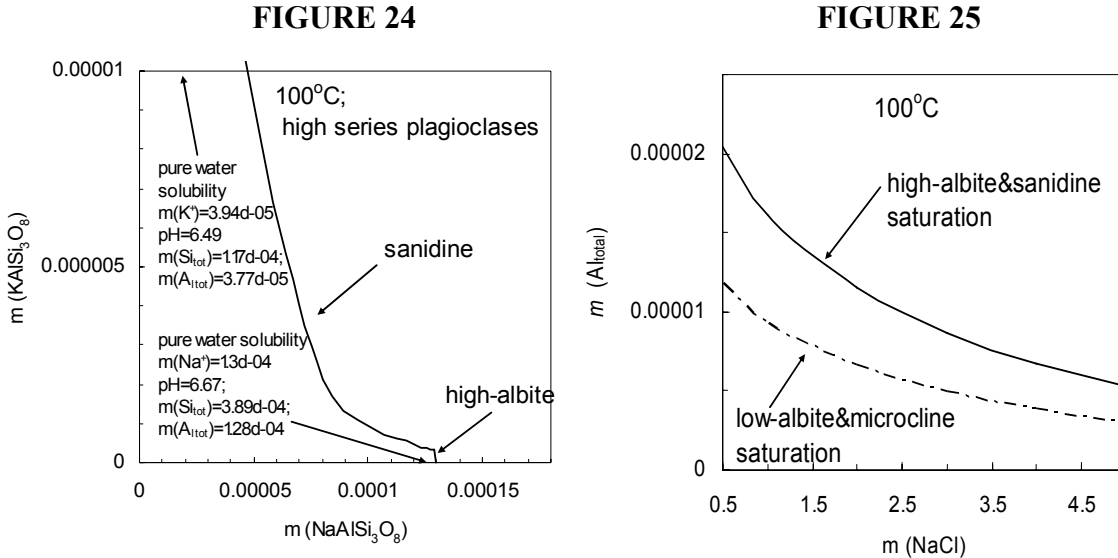


Fig. 24: Solubility in the ternary sandine/high albite ternary.

Fig. 25: Total Al concentration at coexistence in the plagioclase series.

As a further illustration of the capabilities of the model we show in Fig. 26 the solubility diagram for the system  $SiO_2$ , low-albite, microcline,  $H_2O$  at 100°C. Note the dominance of the  $SiO_2$  concentration in most of the diagram. In Fig. 27 we show the model predicted solubility of kaolinite and quartz in pure water as function of pH at 25°C and 150°C and compare the composition of the kaolinite-quartz coexistence point at these temperatures.

In Fig's. 28 and 29 we show the model predicted stability fields of feldspar minerals in the ternary system  $NaAlSi_3O_8$  -  $KAlSi_3O_8$  -  $H_2O$  at 100°C: Fig. 28: low series plagioclases (low-albite & microcline); Fig. 29: high series plagioclases (high-albite & sanidine). The composition of  $MeAlSi_3O_8$  -  $H_2O$  binary solutions is also given inside the figures.

In Fig's. 30 and 31 we show the model prediction of the composition of sodium feldspar-potassium feldspars coexistence points as function of sodium chloride molality and pH at 100°C.

In Fig. 32 we present the calculated composition (as  $Al_{total}$  vs.  $Si_{total}$ ) of solutions saturated with kaolinite at 110°C and constant pH ( $pH \approx 8$ ). Fig. 33 shows the composition of the (kaolinite + boehmite) coexistence point as function of  $Al_{total}$  and pH of solutions.

FIGURE 26

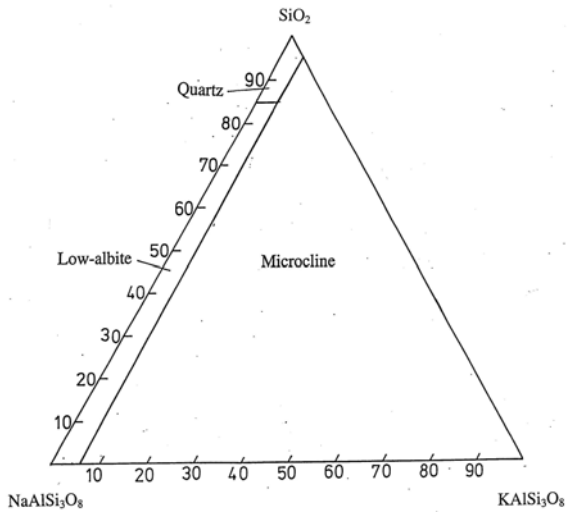


FIGURE 27

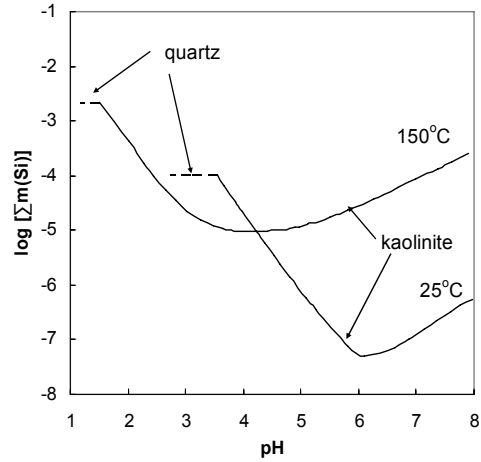


FIGURE 28

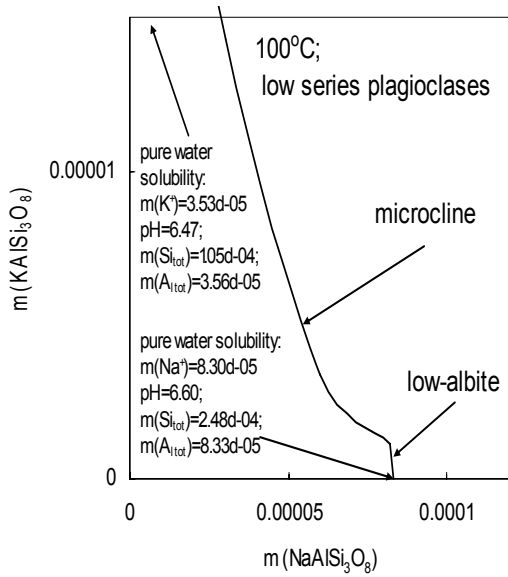
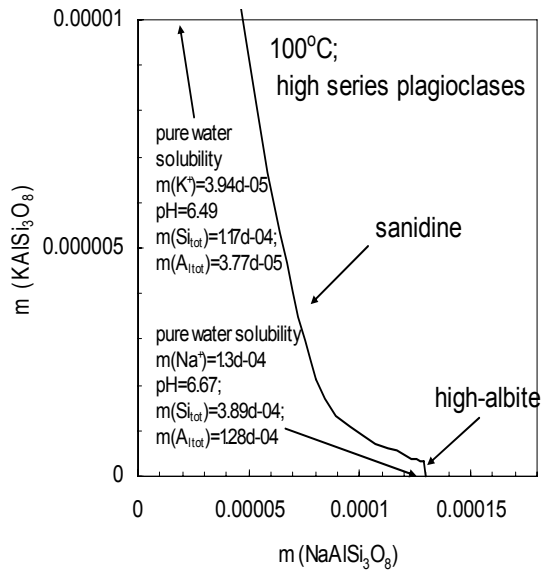
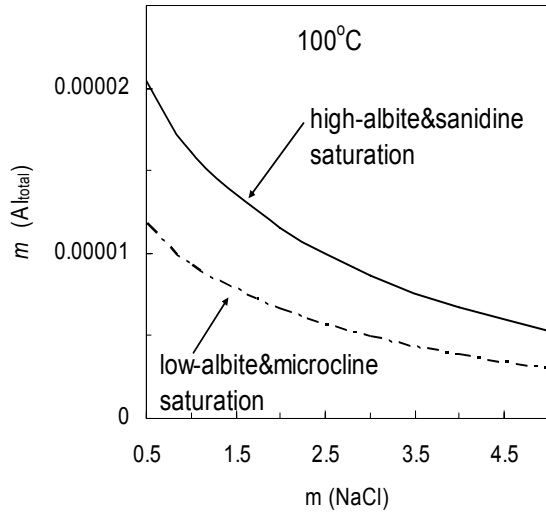


FIGURE 29



**FIGURE 30**



**FIGURE 31**

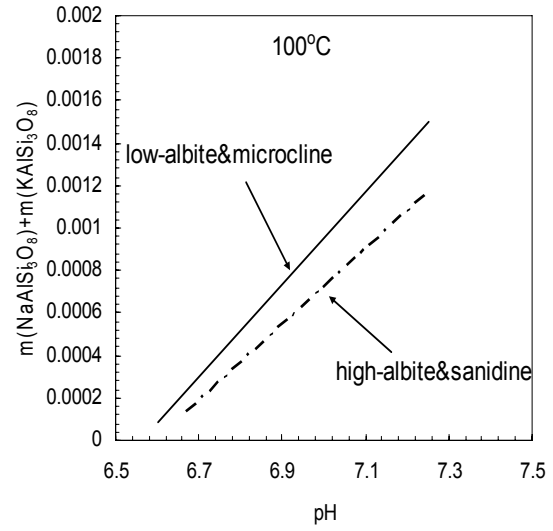


**FIGURE 32**

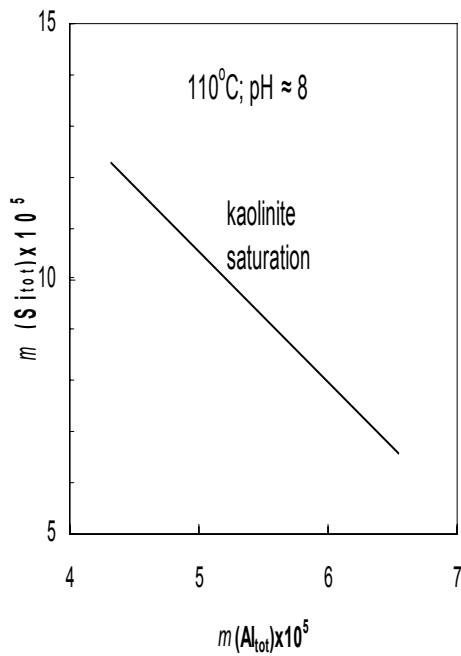
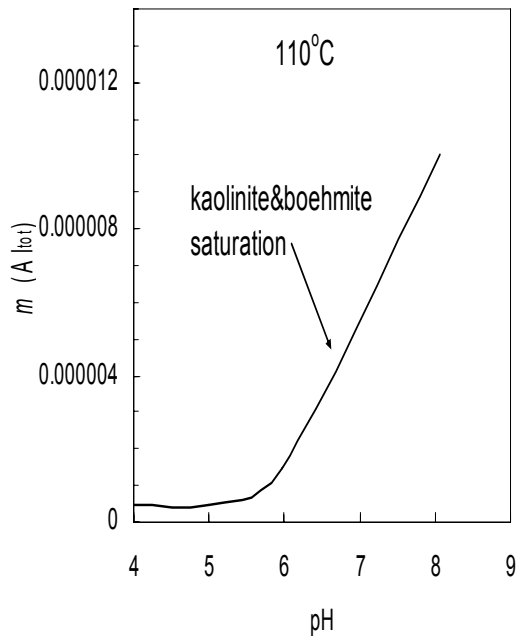


**FIGURE 33**



## 5-5. PROGRESS DEVELOPING AN ISOTHERMAL 25°C MODEL OF THE H-Na-K-Al-Cl-SO<sub>4</sub>-H<sub>2</sub>O SYSTEM

Evidence indicates that the geochemical behavior of aluminum in aqueous systems is modified by interaction with sulfate. Field (e.g., Nordstrom and Ball, 1986) and experimental (e.g., Lydersen et al., 1991; Ridley, 1997) observations have shown that the solubility of aluminum-bearing minerals (such as gibbsite, Al(OH)<sub>3</sub>) is enhanced by the presence of sulfate in natural aqueous solutions. Elevated sulfate concentrations are found in a variety of acidic surface and subsurface waters, including geothermal systems, acid-hypersaline groundwater, acid rain and acid rock drainage. The occurrence of aluminum sulfate minerals has been widely reported. They characterize hydrothermal alteration zones (Nordstrom, 1982), occur in the supergene zone of many ore deposits (Bird et al., 1989) and are also common products of weathering in acid-sulfate environments. An aluminum sulfate model will permit the accurate calculation of the thermodynamic properties of many common hydrothermal minerals (e.g., alunogen, Al<sub>2</sub>(SO<sub>4</sub>)<sub>3</sub>·18H<sub>2</sub>O), sodium alum, Na<sub>2</sub>·Al<sub>2</sub>(SO<sub>4</sub>)<sub>3</sub>·24H<sub>2</sub>O, potassium alum, K<sub>2</sub>·Al<sub>2</sub>(SO<sub>4</sub>)<sub>3</sub>·24H<sub>2</sub>O, alunite, KAl<sub>3</sub>(OH)<sub>6</sub>(SO<sub>4</sub>)<sub>2</sub> and natroalunite, NaAl<sub>3</sub>(OH)<sub>6</sub>(SO<sub>4</sub>)<sub>2</sub>.

We assessed the availability of data to add Al-sulfate/bisulfate interactions to our variable temperature model of pH dependent aluminium hydrolysis and solid/liquid equilibria in the Na-K-H-Cl-OH-Al<sup>3+</sup>-Al(OH)<sup>2+</sup>-Al(OH)<sub>2</sub><sup>+</sup>-Al(OH)<sub>3</sub><sup>0</sup>-Al(OH)<sub>4</sub><sup>-</sup>-H<sub>2</sub>O system. We found few reliable data even in the literature for this task. Therefore we decided to concentrate initially on developing a 25°C model of the interactions of SO<sub>4</sub><sup>2-</sup> and HSO<sub>4</sub><sup>-</sup> species with aluminium hydrolysis species in NaCl and KCl solutions.

There is evidence in the literature of the formation of ion associated species, such as Al(SO<sub>4</sub>)<sup>+</sup>(aq), Al(SO<sub>4</sub>)<sub>2</sub><sup>-</sup>(aq), AlHSO<sub>4</sub><sup>2+</sup>, in aqueous solutions (Ridley et al., 1999; Xiao et al., 2002). However in this initial effort we neglected these species. In constructing this model, the Pitzer parameters for the Na-SO<sub>4</sub> and K-SO<sub>4</sub> binary interactions and for the standard chemical potentials of thenardite (Na<sub>2</sub>SO<sub>4</sub>) and arcanite (K<sub>2</sub>SO<sub>4</sub>) are taken from Greenberg and Moller (1989). The 25°C values for the potassium and sodium acid interactions ( $\theta_{Na,H}$ ,  $\theta_{K,H}$  etc.) are from Christov and Moller (2004a). The  $\beta_{Al,Cl}^0$ ,  $\beta_{Al,Cl}^1$ ,  $C_{Al,Cl}^0$ ,  $\theta_{Na,Al}$ ,  $\theta_{K,Al}$ ,  $\theta_{Al,H}$ ,  $\Psi_{H,Al,Cl}$ ,  $\Psi_{Na,Al,Cl}$  and  $\Psi_{K,Al,Cl}$  parameter values at 25°C are taken from the parameterization of Al<sup>3+</sup> Interactions in the low pH H-Al-Na-K-Cl-H<sub>2</sub>O system (0° to 100°C) (see section 5-2a and Christov et al., 2007).

For this model, we evaluated the Al(hydrolysis species)-SO<sub>4</sub> and Al(hydrolysis species)-HSO<sub>4</sub> binary electrolyte parameters, the acid-aluminum-sulfate mixing parameters and the standard chemical potential of the mineral alunogen (Al<sub>2</sub>(SO<sub>4</sub>)<sub>3</sub>·18H<sub>2</sub>O) using: 1) 25°C osmotic coefficient Al<sub>2</sub>(SO<sub>4</sub>)<sub>3</sub>-H<sub>2</sub>O data up to saturation ( $m^{\max}=1.1$ ); 2) 25°C alunogen solubility data in the Al<sub>2</sub>(SO<sub>4</sub>)<sub>3</sub>-H<sub>2</sub>O binary; and 3) solubilities of alunogen in Al<sub>2</sub>(SO<sub>4</sub>)<sub>3</sub>-H<sub>2</sub>SO<sub>4</sub>-H<sub>2</sub>O mixtures ( $m_{\max}(\text{sat}) = 9 \text{ m H}_2\text{SO}_4$ ).

The sodium ternary interaction,  $\psi_{Na,Al,SO_4}$ , at 25°C was evaluated using solubility data in the Al<sub>2</sub>(SO<sub>4</sub>)<sub>3</sub>-Na<sub>2</sub>SO<sub>4</sub>-H<sub>2</sub>O system at 25°C. The standard chemical potential of the hydrated double salt, sodium alum (Na<sub>2</sub>SO<sub>4</sub>·Al<sub>2</sub>(SO<sub>4</sub>)<sub>3</sub>·24H<sub>2</sub>O-H<sub>2</sub>O), was also obtained from these data. Similarly, the potassium ternary interaction,  $\psi_{K,Al,SO_4}$ , was obtained from solubility data in the Al<sub>2</sub>(SO<sub>4</sub>)<sub>3</sub>-K<sub>2</sub>SO<sub>4</sub>-H<sub>2</sub>O system at 25°C, and potassium alum solubility data were used to evaluate the standard chemical potential of the salt at 25°C.

The predictions of this preliminary model are in reasonable agreement with the low molality (up to about 0.5 *m*) water activity data and the alunogen data at 25°C. In Figure 34 model predictions are compared with the observed solubilities in the  $\text{Al}_2(\text{SO}_4)_3\text{-Na}_2\text{SO}_4\text{-H}_2\text{O}$  ternary at 25°C. Saturation curves in this ternary system are shown for alunogen ( $\text{Al}_2(\text{SO}_4)_3 \cdot 18\text{H}_2\text{O}$  (cr)), mirabilite ( $\text{Na}_2\text{SO}_4 \cdot 10\text{H}_2\text{O}$  (cr)) and the sodium alum,  $\text{Na}_2\text{SO}_4 \cdot \text{Al}_2(\text{SO}_4)_3 \cdot 24\text{H}_2\text{O}$ (cr). The open squares, open triangles and open diamonds show the precipitation of alunogen, sodium alum and mirabilite, respectively. The open circle and closed triangle represent the experimental binary solution  $\text{Na}_2\text{SO}_4 \cdot \text{Al}_2(\text{SO}_4)_3 \cdot 24\text{H}_2\text{O}\text{-H}_2\text{O}$  solubility of sodium alum determined by Mousserson and Gravier (1932) ( $m(\text{sat}) = 0.842$ ) and Smith (1909) ( $m(\text{sat}) = 0.86$ ). The predictions are in good agreement with the experimental data.

Figure 35 for the  $\text{K-Al-SO}_4\text{-H}_2\text{O}$  system is similar to Figure 34, showing three saturation lines corresponding to saturation with respect to alunogen; potassium alum,  $\text{K}_2\text{SO}_4 \cdot \text{Al}_2(\text{SO}_4)_3 \cdot 24\text{H}_2\text{O}$ , and arcanite,  $\text{K}_2\text{SO}_4 \cdot 10\text{H}_2\text{O}$ . In Fig. 35, the 25°C saturation curves predicted by the model (solid line) are compared to the solubility data (open symbols) of Britton (1922). The model predictions are in good agreement with the mixed solution solubility data for potassium sulfate concentrations over 0.08 *m*. The predicted  $m(\text{sat})$  binary solubility of the potassium alum ( $\text{K}_2\text{SO}_4 \cdot \text{Al}_2(\text{SO}_4)_3 \cdot 24\text{H}_2\text{O}$  (cr)) ( $m(\text{sat}) = 0.1599$ ) is also in excellent agreement with the recommended value of Linke (1965) ( $m(\text{sat}) = 0.151$ ) (see closed triangle). However, the predictions of the model for the alunogen + potassium alum invariant point and composition in that region do not agree well with the data. Variations of the  $\psi_{\text{K,Al,SO}_4}$  mixing parameter and of the potassium alum chemical potential did not improve the data fit. Variation of the  $\theta_{\text{Al,K}}$  parameter (taken from the  $\text{SO}_4^{2-}$  free system as above) considerably decreases the good agreement of model predictions with the data in the  $\text{K-Al-Cl-H}_2\text{O}$  system discussed in section 5-2e.

FIGURE 34

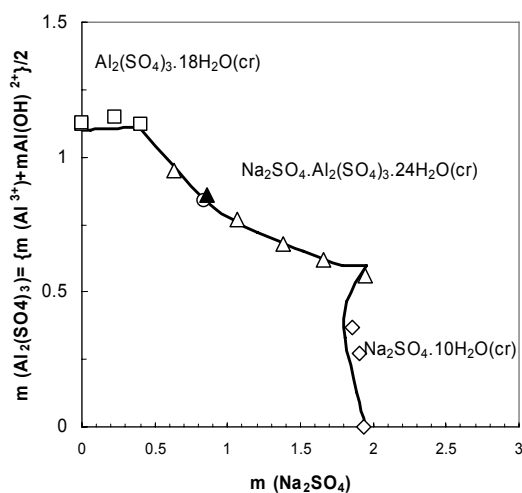
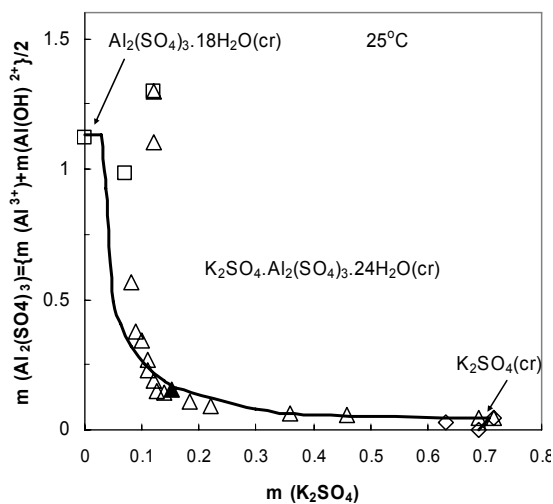


FIGURE 35



## 6. REFERENCES

- Apps J. A., Neil J. M. and Jun C. H. (1989) *Div. Waste Mgt. Office of Nucl. Material Safety and Safeguards, US NRC NUREG/CR-5271-LBL 2148.*
- Arnorsson S. and Stefansson A. (1999) *Am. J. Sci* **299**, 723-751.
- Arnorsson S., Sigurdsson S. and Svavarsson H. (1982) *Geochim. Cosmochim. Acta* **46**, 1513-1532.
- Arnorsson S., Gunnlaugsson E. and Svavarsson H. (1983). *Geochim. Cosmochim. Acta* **47**, 567-577.
- Baes C.F.J. and Mesmer R.E. (1986) *The Hydrolysis of Cations*. Robert Krieger Publishing Co.
- Barany R. and Kelley K. (1961) *U.S. Bur. Mines Rept. Inv.* **5825**.
- Benezeth P., Palmer D. A. and Wesolowski D. J. (2001) *Geochim. Cosmochim. Acta* **65**, 2097-2111.
- Castet S., Dandurand J.-L, Schott J. and Gout R. (1993) *Geochim. Cosmochim. Acta* **57**, 4869-4884.
- Benoit W R. (1987) *Geothermal Resource Council Transactions* **11**, 495-502.
- Bethke C. M. (1996) In: *Geochemical Reaction Modeling: Concepts and Applications*. New York: Oxford University Press, 397.
- Bird M I, Andrew A S, Chivas A R, Lock D E. (1989). *Geochim. Cosmochim. Acta* **53**, 3223.
- Bourcier W., Knauss K. and Jackson K. (1993) *Geochim. Cosmochim. Acta* **57**, 747-762.
- Browne B A, Driscoll C T. (1992). Soluble aluminum silicates: stoichiometry, stability, and implications for environmental geochemistry. *Science* **256**, 1667
- Browne P. R. L. (1978) *Annual Review of Earth and Planetary Science* **6**, 229-250.
- Britton H. (1922) *J. Chem. Soc.*, **121**, 982 (in Linke, 1965, vol. I, p. 216).
- Busey R H. and Mesmer R E. (1977) *Inorganic Chemistry* **16**, 2440-2450..
- Casey W H and Swaddle T W. (2003). *Reviews of Geophysics* **41**.
- Castet S., Dandurand J.-L, Schott J. and Gout R. (1993) *Geochim. Cosmochim. Acta* **57**, 4869-4884.
- Chen C.T. and Marshal W. (1982) *Geochim. Cosmochim. Acta* **46**, 279-287.
- Christov C. and Moller N. (2004a) *Geochim. Cosmochim. Acta* **68**, 1309-1331.
- Christov C. and Moller N. (2004b) *Geochim. Cosmochim. Acta*, **68**, 2004, 3717-3739.



- Christov C., Dickson A. and Moller N. (2007) *J. Solution Chem.* **36**, 1495.
- Devidal J.-L., Dandurand J.-L. and Gout R. (1996) *Geochim. Cosmochim. Acta* **60**, 553-564.
- Deer W A, Howe R A, Zussman J. (1966). *An Introduction to the Rock-Forming Minerals*. London: Longman.
- Department of Energy Specific Plan (1998) DOE Office of Geothermal Technologies.
- Diakonov I., Pokrovski G., Schott J., Castet S. and Gout R. (1996) *Geochim. Cosmochim. Acta* **60**, 197-211.
- Driscoll C T, Schecher W D. (1989). Aqueous Chemistry of Aluminum. In *Aluminum and Health: A Critical Review*, ed. HJ Gitelman, pp. 27. New York, N.Y.: Marcel Dekker, Inc.
- Felmy A. and Weare J. (1986) *Geochim. Cosmochim. Acta* **50**, 2771-2783.
- Fialips C.-I., Majzlan J., Beaufort D. and Navrotsky (2003) *Am. Mineralogist* **88**, 837-845.
- Fournier R O. (1973) Silica in Thermal Waters: Laboratory and Field Investigation, In: Proc. Symp. Hydrogeochem. Biochem., Toyoyo, Japan. Vol 1. The Clarke Co. 122-138.
- Furrer G., Trusch B. and Muller C. (1992) *Geochim. Cosmochim. Acta* **56**, 3831-3838.
- Gmelin's *Handbuch der Anorganischen Chemie, Eisen, Al [B]*, Verlag Chemie G.M.B.H., Berlin, (1932).
- Greenberg J. and Moller N. (1989) *Geochim. Cosmochim. Acta* **53**, 2503-2518.
- Gout R, Pokrovski G S, Schott J, Zwick A. (2000) *J. Soln. Chem.* **29**, 1173
- Gunarsson I. and Arnorsson S. (2000) *Geochim. Cosmochim. Acta* **64**, 2295-2307.
- Harrar J E, Locke F E, Otto C H J, Lorenson L E, Monaco S B and Frey W P. (1982) *J. Soc. Petroleum Engineers* 17-27.
- Harvie C and Weare J H (1980) *Geochim. Cosmochim. Acta* **44**, 981-997.
- Harvie C., Moller N. and Weare J. (1984) *Geochim. Cosmochim. Acta* **48**, 723-751.
- Helgeson H., Delany J., Nesbitt H. and Bird. D. (1978) *Amer. J. Sci.* **278A**, 1-229.
- Hemley J., Montoya J., Marinenko J. and Luce R. (1980) *Econ. Geol.* **75**, 210-228.
- Huang W. (1993) *Chem. Geol.* **105**, 197-214.
- Huang W. and Keller W. (1973) *Amer. Mineral.* **58**, 1023-1028.
- Kastner M. 1971). *Amer. Mineralogist* **56**, 1403
- Kuyunko N., Malinin S. and Khodakovski I. (1983) *Geochem Intl.* **20**, 76-86.
- Linke W., *Solubilities Inorganic and Metal-organic Compounds* 4<sup>th</sup> Ed., vols.

- 1 and 2. Amer. Chem. Soc. Washington (1958, 1965).
- Lydersen E, Salbu B, and Poleo A B S. (1991) *Water Resour. Res.* 27, 351.
- Malquori G (1927a) *Atti Accad. Lincei* **5**, 510; Data given in Linke.
- Malquori G (1927b), *Atti Accad. Lincei* **5**, 576-578; Data given in Linke.
- Malquori G. (1928) *Atti Accad. Lincei* **7**, 740 (1928); Data given in Linke.
- Marshall W L, (1980a) *Geochim. Cosmochim. Acta* **44**, 907-013.
- Marshall W L, (1980b) *Geochim. Cosmochim. Acta* **44**, 925-931.
- Marshall W L and Chen C T A (1982a) *Geochim. Cosmochim. Acta* **46**, 289-291.
- Marshall W L and Chen C T A (1982b) *Geochim. Cosmochim. Acta* **46**, 367-370.
- Marshall W L and Warakowski J M (1980) *Geochim. Cosmochim. Acta* **44**, 915-924.
- Moller N. (1988) *Geochim. Cosmochim. Acta* **52**, 821-837.
- Moller N, Christov C, Weare J H. (2005). *Models of subsurface rock-water processes affecting fluid flow*. Presented at Thirtieth Workshop on Geothermal Reservoir Engineering, Stanford University, Stanford, CA
- Moore, P. B. (1972) "Aluminum," In *Handbook of Geochemistry II-1*, (ed.) K. H. Wedepohl, Springer-Verlag, Berlin, 13-A-1 - 13-O-1.
- Mousseron, M. and Gravier, P. (1932) *Bull. Soc. Chim. France*, **51**, 1382-1387 .
- Mukhamed-Galeev A. and Zotov A. (1992) Report on "Thermodynamics of natural processes" symposium, Novosibirsk, Russia, 13-20 September.
- Nagy K., Blum A. and Lasaga A. (1981). *Amer. J. Sci.* **291**, 649-686.
- Nordstrom D. (1982). *Geochim. Cosmochim. Acta* 46: 681
- Nordstrom D and Ball J W. (1986). *Science* 232: 54
- Palmer D. and Wesolowski, D. (1992) *Geochim. Cosmochim. Acta* **56**, 1093-1111.
- Palmer D. and Wesolowski, D. (1993) *Geochim. Cosmochim. Acta* **57**, 2929-2938.
- Palmer, D., Benezeth P. and Wesolowski, D. (2001) *Geochim. Cosmochim. Acta* **65**, 2081.
- Park H and Englezos P (1999) *Fluid Phase Equilibria* **155**, 251-259.
- Pitzer K S. (1973). *J. Phys. Chem.* **77**, 268.
- Pitzer K S. (1987). In *Reviews in Mineralogy--Thermodynamic Modeling of Geological Materials: Minerals Fluids and Melts*, ed. ISE Carmichael, HP Eugster, pp. 499. Washington, DC: Mineralogical Society of America

- Pitzer KS. (1991) *Activity Coefficients in Electrolyte Solutions*. Boca Raton, FL: CRC Press. 75 pp.
- Reed M. (1989) *Geothermics* **18**, 269-277.
- Ridley M., Wesolowski D J, Palmer D A, Benezeth P, Kettler R. (1997). *Environ. Sci. Technol.*, **31**,1922-1925.
- Ridley M., Wesolowski D J, Palmer D A, and Kettler R. (1999). *Geochim. Cosmochim. Acta* **63**, 459-472.
- Russell A., Edwards J., and Taylor C. (1955) *J. Metals* **7**, 1123-1128.
- Smith W, J. (1909) *Am.Chem. Soc.*, **31**, 245
- Weare J. (1987) Amer. Miner. Soc. Short Course on Thermodynamic Modelling of Geologic Systems, Oct. 26-29, 1987, Phoenix, Arizona.
- Wesolowski D. J. (1992) *Geochim. Cosmochim. Acta* **56**, 1065-1091.
- Wesolowski D. J. and Palmer D. A. (1994) *Geochim. Cosmochim. Acta* **58**, 2947-2969.
- Wilkin R. and Barnes H. (1998). *American Mineralogist* **83**, 746-761.
- Xiao C B, Wesolowski D. J. and Palmer D. A. (1994) *Environ. Sci. Technol.*, **36**,166-173.
- Zotov A., Mukhamet-Galeev A. and Schott J. (1998) *Am. Minerologist* **83**, 516-524.

## 7. STATUS DOE SUPPORTED PITZER MODEL DEVELOPMENT

We have made considerable progress (see Table 4) in completing Pitzer-type models within the comprehensive H-Al-Na-K-Ca-Mg-OH-Cl-HSO<sub>4</sub>-SO<sub>4</sub>-HCO<sub>3</sub>-CO<sub>3</sub>-H<sub>2</sub>O-CO<sub>2</sub>-SiO<sub>2</sub> system that calculate solution activities and solid-liquid-gas equilibria to high solution concentration in the 0° to 250°C temperature range, for pressures along the saturation line. These models can be applied to the prediction of mineral solubility, mineral assemblage stability and acid/base properties in the evaporite, carbonate, silicate and aluminosilicate systems found throughout the earth's surface and crust. The ability to correctly model the solubility of these minerals as a function of fluid composition and temperature is critical to understanding important rock/water and energy production processes affecting fluid flow in geothermal systems (e.g., mineral scaling, rock permeability changes, fluid mixing, the onset of two phase flow) and flashing and scaling in well bores/plant equipment.

<b>Table 4. Status DOE Supported Pitzer Model Development</b>	
<b>Models of solution activities and solid-liquid equilibria</b>	<b>Comments</b>
(1) Model of H-Na-K-Ca-Mg-OH-Cl-HSO <sub>4</sub> -SO <sub>4</sub> -CO <sub>2</sub> -HCO <sub>3</sub> -CO <sub>3</sub> , -H <sub>2</sub> O-CO <sub>2</sub> (gas) 25°C	Harvie, Moller, Weare, 1984
(2) Model Na-K-Ca-Mg-Cl-SO <sub>4</sub> -CO <sub>2</sub> -B(OH) <sub>4</sub> -H <sub>2</sub> O solution activities and solid-liquid equilibria at 25°C	Felmy, Weare, 1986
(3) Model of Na-Ca-Cl-SO <sub>4</sub> -H <sub>2</sub> O solution activities and solid-liquid equilibria, 0°C - 250°C	Moller, 1988
(4) Model of Na-K-Ca-Cl-SO <sub>4</sub> -H <sub>2</sub> O solution activities and solid-liquid equilibria, 0°C - 250°C	Greenberg, Moller, 1989
(5) Model of Na-K-Ca-Mg-Cl-SO <sub>4</sub> -H <sub>2</sub> O solution activities and solid-liquid equilibria, T < 0°C.	Spencer, Moller, Weare, 1990
(6) Model of Na-K-Ca-Mg-Cl-SO <sub>4</sub> -H <sub>2</sub> O solution activities and solid-liquid equilibria, 0°C - 250°C.	Preliminary magnesium interaction model (unpublished)
(7) Model of acid/base H-Na-K-OH-Cl-HSO <sub>4</sub> -SO <sub>4</sub> -H <sub>2</sub> O solution activities and solid-liquid equilibria,, 0°-250°C.	Christov, Moller, 2004a
(8) Model of acid/base H-Na-K-Ca-OH-Cl-HSO <sub>4</sub> -SO <sub>4</sub> -H <sub>2</sub> O solution activities and solid-liquid equilibria,, 0°-250°C.	Christov, Moller, 2004b
(9) Model of silica aqueous chemistry to 250°C.	unpublished.
(10) CO <sub>2</sub> -HCO <sub>3</sub> -CO <sub>3</sub> interactions added to model #7.	Na,K interactions completed, not validated; Preliminary addition of Ca interactions.
(11) Acid aluminum interactions in H-Al-Na-K-Cl-H <sub>2</sub> O system, 0-120°C	Christov, Moller, 2007
(12) Aluminum hydrolysis model of H-Na-K-Al-Cl-OH-Al(OH) <sup>2+</sup> -Al(OH) <sub>2</sub> <sup>+</sup> -Al(OH) <sub>3</sub> <sup>0</sup> -Al(OH) <sub>4</sub> <sup>-</sup> -H <sub>2</sub> O system, NaCl: ≈0-300°C; KCl: ≈0-100°	Manuscript in preparation
(13) Model of silica, aluminum hydroxide and aluminosilicate mineral solubilities to 250°C.	Manuscript in preparation
(14) Aluminum sulfate model of H-Al-Na-HSO <sub>4</sub> -SO <sub>4</sub> -H <sub>2</sub> O, 25°C	Progress on preliminary model

## 8. TECHNOLOGY TRANSFER

To transfer our technology, we have developed an interactive web site (geotherm.ucsd.edu) under previous DOE geothermal grants. Models in three application packages have been incorporated on our web site. To accomplish this, comprehensive user interfaces were developed. Substantial progress has been made on two packages: TEQUIL (rock/water/gas interactions, such as scaling, flashing and reservoir chemistry, as a function of composition to high solution concentration for

temperatures below 300°C) and GEOFLUIDS (multiple phase processes, such as flashing and miscibility, to high T, P supercritical conditions). Some progress has also been made on another package: GEOHEAT (heat characteristics, such as enthalpies, of complex mixtures). This site is accessed by users nationally and internationally. Several validated models have been installed on this web site in the past but funding has not been available to update this web site (user codes, user documentation and new validated models).

Publications of our research results (see section 8 below) have also reached a world wide audience. Consequently, our chemical model technologies, which have wide application to many energy related and other important problems (e.g., scaling prediction in petroleum production systems, stripping towers for mineral production processes, nuclear waste storage, CO<sub>2</sub> sequestration strategies, global warming), have been incorporated in many model packages both in the United States and in other countries (e.g., TEQUIL, EQ3/6NR, PHREEQ, GMIN, REACT, FLOTRAN, FREEZCHEM, ESP, TUFFREACT, SCAPE2). Our 25°C model (Table 1, model#1) provided the basis for the implementation of Pitzer type models in widely distributed software packages (e.g., EQ3NR(258) (LLNL) and PHRQPITZ(195)(USGS)) and in atmospheric models.

## 9. DOE RELATED PUBLICATIONS

Listed below are forty articles on DOE related research that have been published in peer-reviewed journals and in conference proceedings. Several are in preparation. Our work has also been presented at many workshops and conferences.

- Stuart Bogatko, Eric J. Bylaska, and John H. Weare, 1<sup>st</sup> principles Simulation of the Bonding, Vibrational, and Electronic Properties of the Hydration Shells of High Spin Fe<sup>3+</sup>, submitted for publication.
- Eric J. Bylaska, Marat Valiev, James R. Rustad, and John H. Weare, (2007) Structures of the Hydration Shells of the Al<sup>3+</sup> Ion. *The Journal of Chemical Physics*, **126**, 104505.
- Brantley S., Crerar D., Moller N., and Weare J. H. (1984) Geochemistry of a marine evaporite: Bocana de Virilla, Peru. *J. Sediment. Petrol.* **54**, 447-462.
- Christov C. and Moller N. (2004a) Chemical equilibrium model of solution behavior and solubility in the H-Na-K-OH-Cl-HSO<sub>4</sub>-SO<sub>4</sub>-H<sub>2</sub>O system to high concentration and temperature. *Geochimica et Cosmochimica Acta* **68**(6), 1309-1331.
- Christov C. and Moller N. (2004b) A chemical equilibrium model of solution behavior and solubility in the H-Na-K-Ca-OH-Cl-HSO<sub>4</sub>-SO<sub>4</sub>-H<sub>2</sub>O system to high concentration and temperature. *Geochimica et Cosmochimica Acta* **68**(18), 3717-3739.
- Christov C. Dickson A. and Moller N. (2007) Thermodynamic modeling of aqueous aluminum chemistry and solid-liquid equilibria to high solution concentration and temperature. I. The acidic H-Al-Na-K-Cl-H<sub>2</sub>O system from 0° to 100°C. *J. Solution Chem.* **36**, 1495.
- Duan Z., Moller N., and Weare J. H. (2001) Monte Carlo Gibbs ensemble simulation of phase equilibria of the RWK2 water. *Abstracts of Papers - American Chemical Society*.

- Duan Z., Moller N., and Weare J. H. (2006) A high temperature equation of state for the H<sub>2</sub>O-CaCl<sub>2</sub> and H<sub>2</sub>O-MgCl<sub>2</sub> systems. *Geochimica et Cosmochimica Acta* **70**(15), 3765-3777.
- Duan Z. H., Moller N., Derocher T., and Weare J. H. (1996a) Prediction of boiling, scaling and formation conditions in geothermal reservoirs using computer programs *TEQUIL* and *GEOFLUIDS*. *Geothermics* **25**(6), 663-678.
- Duan Z. H., Moller N., Greenberg J., and Weare J. H. (1992a) The prediction of methane solubility in natural waters to high ionic strength from 0 to 250°C and from 0 to 1600 bar. *Geochimica et Cosmochimica Acta* **56**(4), 1451-1460.
- Duan Z. H., Moller N., and Weare J. H. (1992b) An equation of state for the CH<sub>4</sub>-CO<sub>2</sub>-H<sub>2</sub>O System: I. Pure systems from 0 to 1000°C and 0 to 8000 bar. *Geochimica et Cosmochimica Acta* **56**(7), 2605-2617.
- Duan Z. H., Moller N., and Weare J. H. (1992c) An equation of state for the CH<sub>4</sub>-CO<sub>2</sub>-H<sub>2</sub>O System: II. Mixtures from 50 to 1000°C and 0 to 1000 bar. *Geochimica et Cosmochimica Acta* **56**(7), 2619-2631.
- Duan Z. H., Moller N., and Weare J. H. (1992d) Molecular dynamics simulation of PVT properties of geological fluids and a general equation of state of nonpolar and weakly polar gases up to 2000 K and 20,000 bar. *Geochimica Et Cosmochimica Acta* **56**(10), 3839-3845.
- Duan Z. H., Moller N., and Weare J. H. (1995a) Equation of state for the NaCl-H<sub>2</sub>O-CO<sub>2</sub> System: Prediction of phase equilibria and volumetric properties. *Geochimica et Cosmochimica Acta* **59**(14), 2869-2882.
- Duan Z. H., Moller N., and Weare J. H. (1995b) Measurement of the PVT properties of water to 25 Kbars and 1600°C from synthetic fluid inclusions in corundum - comment. *Geochimica et Cosmochimica Acta* **59**(12), 2639-2639.
- Duan Z. H., Moller N., and Weare J. H. (1995c) Molecular dynamics equation of state for nonpolar geochemical fluids. *Geochimica et Cosmochimica Acta* **59**(8), 1533-1538.
- Duan Z. H., Moller N., and Weare J. H. (1995d) Molecular dynamics simulation of water properties using RWK2 potential - from clusters to bulk water. *Geochimica et Cosmochimica Acta* **59**(16), 3273-3283.
- Duan Z. H., Moller N., and Weare J. H. (1996b) Equation of state for the NH<sub>3</sub>-H<sub>2</sub>O system. *Journal of Solution Chemistry* **25**(1), 43-50.
- Duan Z. H., Moller N., and Weare J. H. (1996c) A general equation of state for supercritical fluid mixtures and molecular dynamics simulation of mixture PVTX properties. *Geochimica et Cosmochimica Acta* **60**(7), 1209-1216.
- Duan Z. H., Moller N., and Weare J. H. (1996d) Prediction of the solubility of H<sub>2</sub>S in NaCl aqueous Solution: an equation of state approach. *Chemical Geology* **130**(1-2), 15-20.
- Duan Z. H., Moller N., and Weare J. H. (2000) Accurate prediction of the thermodynamic properties of fluids in the system H<sub>2</sub>O-CO<sub>2</sub>-CH<sub>4</sub>-N<sub>2</sub> up to 2000 K and 100 kbar from a corresponding states/one fluid equation of state. *Geochimica et Cosmochimica Acta* **64**(6), 1069-1075.
- Duan Z. H., Moller N., and Weare J. H. (2003) Equations of state for the NaCl-H<sub>2</sub>O-CH<sub>4</sub> system and the NaCl-H<sub>2</sub>O-CO<sub>2</sub>-CH<sub>4</sub> system: Phase equilibria and volumetric properties above 573 K. *Geochimica et Cosmochimica Acta* **67**(4), 671-680.

- Duan Z. H., Moller N., and Weare J. H. (2004) Gibbs ensemble simulations of vapor/liquid equilibrium using the flexible RWK2 water potential. *Journal of Physical Chemistry B* **108**(52), 20303-20309.
- Eugster H. P., Harvie C. E., and Weare J. H. (1980) Mineral equilibria in a six-component seawater system, Na-K-Ca-SO<sub>4</sub>-Cl-H<sub>2</sub>O, at 25°C. *Geochimica et Cosmochimica Acta* **44**, 1335-1347.
- Felmy A. R. and Weare J. H. (1986) The prediction of borate mineral equilibria in natural waters: application to Searles Lake, California. *Geochimica et Cosmochimica Acta* **50**, 2771-2783.
- Felmy A. R. and Weare J. H. (1991a) Calculation of Multicomponent Ionic Diffusion from Zero to High Concentration .1. the System Na-K-Ca-Mg-Cl-SO<sub>4</sub>-H<sub>2</sub>O at 25°C. *Geochimica et Cosmochimica Acta* **55**(1), 113-131.
- Felmy A. R. and Weare J. H. (1991b) Calculation of Multicomponent Ionic Diffusion from Zero to High Concentration .2. Inclusion of Associated Ion Species. *Geochimica et Cosmochimica Acta* **55**(1), 133-144.
- Greenberg J. P., Weare J. H., and Harvie C. E. (1985) An equilibrium computation algorithm for complex highly nonideal systems. Application to silicate phase equilibria. *High Temperature Science* **20**, 141-162.
- Harvie C., Greenberg J. P., and Weare J. H. (1987) A chemical equilibrium algorithm for highly non-ideal multiphase systems: Free energy minimization. *Geochimica et Cosmochimica Acta* **51**, 1045-1057.
- Harvie C., Moller N., and Weare J. (1984) The prediction of mineral solubilities in natural waters: The Na-K-Mg-Ca-H-Cl-SO<sub>4</sub>-OH-HCO<sub>3</sub>-CO<sub>3</sub>-CO<sub>2</sub>-H<sub>2</sub>O system from zero to high concentration at 25 C. *Geochimica et Cosmochimica Acta* **48**, 723-751.
- Harvie C., Weare J. H., Hardie L. A., and Eugster H. P. (1980) Evaporation of seawater: Calculated mineral sequences. *Science* **208**, 498-500.
- Harvie C. E., Eugster H. P., and Weare J. H. (1982) Mineral Equilibria in the 6-Component Sea-Water System, Na-K-Mg-Ca-SO<sub>4</sub>-Cl-H<sub>2</sub>O at 25-Degrees-C .2. Compositions of the Saturated Solutions. *Geochimica et Cosmochimica Acta* **46**(9), 1603-1618.
- Harvie C. E. and Weare J. H. (1980) The prediction of mineral solubilities in natural waters: The Na-K-Mg-Ca-Cl-SO<sub>4</sub>-H<sub>2</sub>O systems from zero to high concentration at 25°C. *Geochim. Cosmochim. Acta* **44**, 981-997.
- Mingyan Li, Zhenhao Duan, Zhigang Zhang, Chi Zhang and John Weare, The Structural and Dynamics Properties of CaCl<sub>2</sub>(aq) for Wide Concentration at Ambient and High Temperature by Molecular Dynamics Simulation, submitted for publication.
- Moller N. (1988) The prediction of mineral solubilities in natural waters: a chemical equilibrium model for the Na-Ca-Cl-SO<sub>4</sub>-H<sub>2</sub>O system to high temperature and concentration. *Geochimica et Cosmochimica Acta* **52**, 821-837.
- Moller N., Christov C., and Weare J. H. (2005) Models of subsurface rock-water processes affecting fluid flow. *Thirtieth Workshop on Geothermal Reservoir Engineering, Stanford University, Stanford, CA*.
- Moller N., Christov C., and Weare J. (2006) Thermodynamic Models of Aluminum Silicate Mineral Solubility for Application to Enhanced Geothermal Systems. *The Thirty-first Workshop on Geothermal Reservoir Engineering, Stanford University, Stanford, CA, January 30-February 1, 2006*.

- Moller N., Christov C., and Weare J. (2007) Thermodynamic Model for Predicting Interactions of Geothermal Brines With Hydrothermal Aluminum Silicate Minerals. *The Thirty-Second Workshop on Geothermal reservoir Engineering, Stanford University, Stanford, CA. January 22-23, 2007.*
- Weare J. H., Moller N., Duan Z. H., and Christov C. (2001) Thermodynamic models of natural fluids: Theory and practice. *Abstracts of Papers of the American Chemical Society* **221**, U535-U536.
- Spencer R. J., Moller N., and Weare J. (1990) Predictions of mineral solubilities in natural waters: a chemical equilibrium model for the Na-K-Ca-Mg-Cl-SO<sub>4</sub>-H<sub>2</sub>O system at temperatures below 25°C. *Geochimica et Cosmochimica Acta* **54**, 575-590.

In addition, we have made considerable progress in completing the research for manuscripts describing the (1) the model of aluminum hydrolysis in the H-Na-K-Al-Cl-OH-Al(OH)<sup>2+</sup>-Al(OH)<sub>2</sub><sup>+</sup>-Al(OH)<sub>3</sub><sup>0</sup>- Al(OH)<sub>4</sub><sup>-</sup>-H<sub>2</sub>O system, (NaCl: ≈0-300°C; KCl: ≈0-100°C); (2) the model of silica, aluminum hydroxide and aluminosilicate mineral solubilities to 250°C and the (3) the model of CO<sub>2</sub>-HCO<sub>3</sub><sup>-</sup>-CO<sub>3</sub><sup>2-</sup> interactions in H-Na-K-OH-Cl-HSO<sub>4</sub><sup>-</sup>-SO<sub>4</sub><sup>2-</sup>-H<sub>2</sub>O system to 250°C. (4) 1<sup>st</sup> Principle Simulation of Hydration Shell Dynamics and Ligand Exchange in the CaCl<sub>2</sub>-H<sub>2</sub>O system, in preparation. (5) 1<sup>st</sup> Principle Simulation of High Temperature Ion Association CaCl<sub>2</sub>-H<sub>2</sub>O system, in preparation.

## 10. RELEVANT QUALIFICATIONS AND PAST EXPERIENCE OF UCSD TEAM MEMBERS

The research program proposed for DOE grant DE-FG36-04GO14300 reflects many years of active geothermal-related research in chemical modeling and communication with geothermal industry, researchers and the Department of Energy. The team working on this DOE grant included:

Nancy Moller, Principal Investigator: Ph.D. in Earth Science, 27 years of experience in chemical modeling, many publications related to chemical modeling and the application of thermodynamics to natural, geothermal and industrial processes. Senior Research Chemist, NSF Postdoctoral Fellow in Energy Related Science.

John Weare, Coprincipal Investigator: Ph.D. in Chemical Physics, 35 years of experience in thermodynamic theory, many publications in thermodynamics and related areas, Professor of Chemistry, Senior Fellow San Diego Supercomputer Center.

Both investigators have, separately or together, managed many federally funded (e.g., DOE, NSF, ONR, AFSOR, PRF) research programs.

Christomir Christov, Project Scientist: Ph. D. Chemistry, 20 years experience in aqueous solution study (experimental and thermodynamic modeling).